SKBF
KBS
TEKNISK
RAPPORT
83-38

Evaluation of some tracer tests in the granitic rock at Finnsjön

L Moreno
I Neretnieks

Royal Institute of Technology, Stockholm

C-E Klockars

Swedish Geological, Uppsala April 1983

SVENSK KÄRNBRÄNSLEFÖRSÖRJNING AB / AVDELNING KBS

POSTADRESS: Box 5864, 102 48 Stockholm, Telefon 08-67 95 40

EVALUATION OF SOME TRACER TESTS IN GRANITIC ROCK AT FINNSJÖN

Luis Moreno
Ivars Neretnieks

Royal Institute of Technology, Stockholm

Carl-Erik Klockars
Swedish Geological, Uppsala
April, 1983

EVALUATION OF SOME TRACER TESTS IN GRANITIC ROCK AT FINNSJÖN

Luis Moreno
Ivars Neretnieks
Carl-Erik Klockars

EVALUATION OF SOME TRACER TESTS IN GRANITIC ROCK

AT FINNSJÖN

Contents

Summary
Introduction and aims
Mechanisms
Models and methods of solution
Fitting of data to models
Results
Discussion
Conclusions
Nomenclature
References
Appendices

Luis Moreno*
Ivars Neretnieks*
Carl-Erik Klockars**

* Royal Institute of Technology
Department of Chemical Engineering
Stockholm, Sweden.

** Swedish Geological
Uppsala, Sweden.

SUMMARY

Tracer tests in a granitic rock have been analysed. A nonsorbing tracer - iodide - was used to investigate the hydraulic properties of the pathway. This gives the mean residence time(s) and spreading. The latter may be caused by channeling, hydrodynamic dispersion and interaction with the matrix. Four different models emphasizing different combinations of the various mechanisms were used.

It was found that even the nonsorbing tracer interacts considerably with the matrix. Recent laboratory data which show a high porosity of fissure coating materials indicate that the cause for this interaction may be diffusion of the tracer into the pore water of the matrix.

The residence time(s) and dispersion data obtained from the iodide test were used to predict the behaviour of the sorbing tracer strontium. Independent laboratory data for strontium sorption and diffusion in granite were used in the predictions. The predicted data were in very poor agreement with the field data. The field data were then used to fit the model parameters. The resulting combination of sorption and diffusion data which gives a good fit to the field data was off by a few orders of magnitude.

An examination of some recent sorption and diffusion data show that at the high concentration, which was used in the field test, the sorption isotherm is nonlinear and the sorption capacity considerably smaller than that used in the original predictions. The new data would account for the lower retardation. As, however, the new sorption data have not been performed on the actual fissure coating material in the flowpath and no diffusion measurements at very high concentrations have yet been performed the conclusions are only tentative.

1.0 INTRODUCTION AND AIMS

In the Swedish studies (KBS Nuclear Fuel Safety project), crystalline rock has been selected as the most suitable bedrock in which to build a final repository for spent nuclear fuel. The radioactive wastes from nuclear power plants would be placed at a depth of about 500 m. If a canister containing radioactive waste is destroyed, water flowing in the bedrock will come in contact with the radioactive material. The radionuclides carried by the water may interact in various ways with the rock. They may be retarded by sorption onto the surface of the fissures and microfissures and by diffusion into the rock matrix. This last mechanism is an important factor in the retardation of radionuclides (Neretnieks, 1980). The tracers penetrate into the microfissures and they may be adsorbed within the matrix.

The prediction of the behaviour of a radioactive subtance, when flowing through a fissured medium, depends on knowledge of the sorption capacity of the rock and the effective diffusion of the tracer into the matrix. These parameters for granite have been determined in the laboratory (Allard et al. 1978; Skagius et al. 1982 and Skagius and Neretnieks, 1982)

In situ experiments have been performed and are used to test the predictions made by laboratory data. In these experiments nonsorbing substances were used to determine the hydraulic properties. In Sweden various field experiments have been performed (Landström et al. 1978; Gustafsson and Klockars, 1981 and Landström et al., 1983).

This report aims at testing several models for tracer transport in fissured rock with experimental data from the Finnsjö area (Gustafsson and Klockars, 1981), and to compare the results with independent laboratory data. Two interacting mechanisms are of special interest as they have a strong impact on the transport of radionuclides in the geosphere. They are hydrodynamic dispersion or channeling and the penetration of the rock matrix by diffusion.

The approach taken is to use the nonsorbing tracer to determine the hydraulics of the system and then to attempt to predict the migration of the sorbing tracer using independently obtained sorption and matrix diffusion data.

2.0 EXPERIMENTS

The tracer tests were made in granitic rock at a depth of about 100 meters. Tracers were injected in one bore hole between two packers straddling a high permeability zone. In another hole 30 m distant a pump was continuously withdrawing water with the aim of creating a drawdown zone into which all the tracers from the injection would eventually flow. The difference in hydraulic head varied from 6.0 to 7.6 m in the different runs. Data for these runs are found in the Intracoin letter (working group on collection of in-situ data) of 1982-01-15. The experimental procedure is described by Gustafsson and Klockars (1981). The location of the injection and pumping holes are shown in figure 1. The run with continuous injection for 350 hours will be studied. In this run a nonsorbing substance (iodide) was injected simultaneously with a sorbing tracer (strontium). The experimental data is presented in Appendix A.

Sorption equilibria constant for Finnsjö granite have been measured by Skagius et al. (1982). The sorption data were obtained on particles with different sizes, which made it possible to evaluate the sorption capacity on the outer surfaces of the particles as well as the sorption capacity of the internal surfaces.

The diffusivity of strontium in crushed granite particles was measured by Skagius et al.(1982) by means of a long time contact experiment with granite particles and liquid with tracer. The sorption equilibrium constants and effective diffusion coefficients for cesium and strontium in pieces of granite have been determined by Skagius and Neretnieks (1982). The effective diffusion coefficient for iodide in pieces of granite is also presented in that report.

The experimental conditions of the tracer test and the values determined in the laboratory are shown in table 2.1. The tracer test results are shown in figure 2.

Gustafsson and Klockars (1981) determined that the tracer solution is diluted 5 times in the pumping well, due to water flow from other levels. This value has been used in the calculation of fissure widths.

Table 2.1

Data for the tracer runs at Finnsjö, and sorption and diffusion data of granite.

Injected tracer			iodide and strontium
Injection rate	l/s		$2.7 \cdot 10^{-4}$
concentration of injected solution	mol/l	I	$6.7 \cdot 10^{-2}$
		Sr	$9.4 \cdot 10^{-2}$
Pumping rate	l/s		0.1
Difference in hydraulic head	m		6.7
Distance between injection and pumping points	m		30
Hole diameters	m		0.11
Mass sorption coefficient*	m^3/ton	K_d(Sr)	7.4
Surface sorption coefficient*	m	K_a(Sr)	$7.0 \cdot 10^{-5}$
Effective Diffusivity	m^2/s	D_e(I)	$0.08 \cdot 10^{-12}$
Effective Diffusivity*	m^2/s	D_e(Sr)	$24.0 \cdot 10^{-12}$
Density of Finnsjö granite	ton/m^3		2.7
Porosity of rock matrix	m^3/m^3		0.003
Mass sorption coefficient**	m^3/ton	K_d(Sr)	2.7
Effective Diffusivity**	m^2/s	D_e(I)	$0.10 \cdot 10^{-12}$
Effective Diffusivity**	m^2/s	D_e(Sr)	$2.20 \cdot 10^{-12}$

(*) Values determined for crushed granite 0.1-5 mm particles with concentrations around 5 ppm in the water.

(**) Values determined for sawed pieces of granite, concentrations around 5 ppm in the water.

3.0 MECHANISMS

When a tracer flows through porous or fissured media. it will be dispersed. There are many mechanisms contributing to such spreading:

- o molecular diffusion in the liquid
- o velocity variations in the fluid in a channel
- o velocity variations between channels in a porous or fissured medium
- o chemical or physical interactions with the solid material.

Spreading by molecular diffusion results from variations in tracer concentration within the liquid phase. Because the molecular diffusion effects depend on time, their effects on the overall dispersion will be more significant at low flow velocities. In flow through fissured media, molecular diffusion occurs into the solid matrix through the microfissures. The molecular diffusion in the liquid in the fissures in the direction of the flow is negligible compared to the mechanical dispersion in the in situ experiments.

Mechanical dispersion is caused by the local variations in velocity, both in magnitude and direction. The velocity variations are assumed to be of random nature. In a porous medium the differences in pore sizes, lengths and orientations cause the velocity variations.

Bear (1969) gives a comprehensive review of hydrodynamic dispersion theories. Hydrodynamic dispersion includes mechanical dispersion and molecular diffusion. Mathematically, it is treated in the same way as molecular diffusion.

Channeling dispersion occurs when a tracer flows through non-interconnected channels with different velocities. The velocity differences of the liquid in the channels will carry a tracer different distances over a given time.

In flow through fissured media, examples of interactions with the matrix are the sorption onto the surface of the fissure and the sorption within the rock matrix.

4.0 PRESENTATION OF THE MODELS AND METHOD OF SOLUTION

In the preceding part the different mechanisms which may exist when a tracer flows through a fissure have been presented. The proposed models include some of these mechanisms. The following models have been tested:

- o Hydrodynamic dispersion in several pathways model
- o Hydrodynamic dispersion-diffusion model
- o Channeling dispersion-diffusion model
- o Hydrodynamic dispersion-diffusion and stagnant water model.

The hydrodynamic dispersion-diffusion model is also extended from a one-pathway to a two-pathway model. This extension is presented in Appendix B.

4.1 General

According to Lenda and Zuber (1970), the radial convergent flow in these experiments may be represented by the equations for linear flow. Sauty (1980) pointed out that this relationship is adequate when the Peclet number is greater than 3. The equations will be written for linear flow.

For one-dimensional flow in a channel, the transport of a tracer is given by

$$\frac{\partial C_f}{\partial t} + U_f \frac{\partial C_f}{\partial x} - D_L \frac{\partial^2 C_f}{\partial x^2} + f(C_f,..,) = 0 \qquad (4.1.1)$$

The term $f(C_f,...,)$ accounts for reactions of the tracer within the flowing fluid or with the solid of the matrix. In the case of surface reaction the equation may be written as

$$\frac{\partial C_f}{\partial f} + \frac{2}{\delta} \frac{\partial C_s}{\partial t} + U_f \frac{\partial C_f}{\partial x} - D_L \frac{\partial^2 C_f}{\partial x^2} = 0 \qquad (4.1.2)$$

In this equation, U_f corresponds to the average fluid velocity between the injection and pumping holes.

Assuming a linear equilibrium reaction between the tracer concentration in the fluid and the tracer concentration adsorbed on the surface of the solid

$$C_s = K_a \cdot C_f \qquad (4.1.3)$$

and thus

$$\frac{\partial C_s}{\partial t} = K_a \frac{\partial C_f}{\partial t} \qquad (4.1.4)$$

The equation (4.1.2) becomes

$$R_a \frac{\partial C_f}{\partial t} + U_f \frac{\partial C_f}{\partial x} - D_L \frac{\partial^2 C_f}{\partial x^2} = 0 \qquad (4.1.5)$$

where R_a is the surface retardation factor, which is defined as

$$R_a = 1 + \frac{2}{\delta} K_a \qquad (4.1.6)$$

For a bulk reaction where the solid is penetrated throughout, the volume retardation factor is defined as

$$R_d = 1 + \frac{1-\varepsilon_p}{\varepsilon_p} K_d' \rho_s \qquad (4.1.7)$$

Where K_d' is the volume equilibrium constant between the tracer concentration in the pore fluid and the tracer concentration within the solid

$$C_m = K_d' \cdot C_p \qquad (4.1.8)$$

In this case K_d' is based on the mass of the solid proper.

The definition of the volume equilibrium constant is sometimes based on the mass of the microfissured solid and includes the nuclide which is in the water in the microfissures as well as that in the solid

$$K_d \rho_p = \varepsilon_p + (1-\varepsilon_p) K_d' \rho_s \qquad (4.1.9)$$

and the volume retardation factor may be written as

$$R_d = \frac{K_d \rho_p}{\varepsilon_p} \qquad (4.1.10)$$

For a nonsorbing substance ($K_d' = 0$), the porous rock matrix still has a sorption equilibrium constant equal to ε_p/ρ_p due to the concentration of tracer in the pores.

4.2 Governing equations for the flow rate

In the tracer test with radial flow through a fissure the hydraulic conductivity of the fissure is determined by integration of Darcy's equation

$$K_{pf} = \frac{1}{2} \frac{\ln (\frac{r_2}{r_1})(r_2^2-r_1^2)}{(h_2-h_1)\ t_w} \qquad (4.2.1)$$

The radial velocity in the fissure at radius r may be calculated from

$$U_r = \frac{1}{r} \frac{(h_2-h_1)}{\ln (r_2/r_1)} K_{pf} \qquad (4.2.2)$$

If the water residence time is known. the water velocity may be evaluated directly by means of

$$U_r = \frac{1}{2r} \frac{(r_2^2-r_1^2)}{t_w} \qquad (4.2.3)$$

and the fissure width may be expressed as

$$\delta_f = \frac{Q \cdot t_w}{\pi(r_2^2-r_1^2)} \qquad (4.2.4)$$

where Q is the flow rate through the fissure.

The hydraulic conductivity may be used to determine an equivalent "Flat channel laminar flow fissure width". This is the width of a channel with parallel walls which would give the same resistence to the flow as the actual fissure. This width is expressed as

$$\delta_l = \sqrt{K_{pf} \cdot \frac{12\ \upsilon}{g}} \qquad (4.2.5)$$

4.3 Hydrodynamic dispersion in several pathways model

This model considers a case where the transport of the tracers from the point of injection to the point of pumping takes place through separate parallel fissures. There is no connection between the different pathways.

The interaction between the tracer and the solid material is limited only to the walls of the fissures (surface sorption mechanism). The following mechanisms are included in the model:

- o Advective transport along the fissure
- o Hydrodynamic dispersion in the direction of the flow in the fissure
- o Adsorption onto the surface of the fissure.

The governing equation for the tracer concentration in the pumping hole may be written from equation (4.1.1) including the surface sorption mechanism as

$$\frac{\partial C_f}{\partial f} + \frac{2}{\delta}\frac{\partial C_s}{\partial t} + U_f \frac{\partial C_f}{\partial x} - D_L \frac{\partial^2 C_f}{\partial x^2} = 0 \qquad (4.3.1)$$

Introducing the surface retardation factor defined in (4.1.6) the equation (4.3.1) becomes

$$R_a \frac{\partial C_f}{\partial f} + U_f \frac{\partial C_f}{\partial x} - D_L \frac{\partial^2 C_f}{\partial x^2} = 0 \qquad (4.3.2)$$

the initial and boundary conditions are

$$\begin{aligned} C_f(x,0) &= 0 \\ C_f(0,t) &= C_0 \\ C_f(\infty,t) &= 0 \end{aligned} \qquad (4.3.3)$$

The solution for the differential equation with its corresponding initial and boundary conditions is given by Ogata and Banks (1961)

$$C_f = \frac{C_o}{2}\left[\text{erfc}\ \frac{Pe^{0.5}(1-t_R)}{2\ t_R^{0.5}} + e^{Pe}\ \text{erfc}\ \frac{Pe^{0.5}(1+t_R)}{2\ t_R^{0.5}}\right] \qquad (4.3.4)$$

where

$t_R = t/t_o$

$Pe = U_f \cdot x/D_L$

$t_o = R_a \cdot t_w$

4.4 Hydrodynamic dispersion-diffusion model

In the preceding model only the interaction of the tracer with the surface of the walls of the fissure was included. This model includes the interaction of the tracer with the rock matrix as well.

It is assumed that the transport of the tracers takes place through a single fissure. The tracers penetrate into the rock matrix by molecular diffusion and they may be adsorbed onto the fracture surface and within the rock matrix.

The model considers the transport of contaminants in a fluid that flows through a thin fracture situated in a water-saturated porous rock. The groundwater velocity in the fracture is assumed constant. The following processes will be considered:

- o Advective transport along the fracture
- o Longitudinal mechanical dispersion in the fracture
- o Molecular diffusion from the fracture into the rock matrix
- o Adsorption onto the surface of the fracture
- o Adsorption within the rock matrix.

In this case equation (4.1.1) must include the surface sorption mechanism as well as the flux perpendicular to the fissure axis due to the diffusion into the rock matrix

$$\frac{\partial C_f}{\partial t} + \frac{2}{\delta}\frac{\partial C_s}{\partial t} + U_f \frac{\partial C_f}{\partial x} - D_L \frac{\partial^2 C_f}{\partial x^2} - D_e \frac{2}{\delta}\frac{\partial C_p}{\partial z}\bigg|_{z=0} = 0$$

$$0 \leq x \leq \infty \qquad (4.4.1)$$

Assuming a linear equilibrium isotherm for the surface sorption and using the surface retardation coefficient R_a the differential equation for the fissure becomes

$$\frac{\partial C_f}{\partial t} - \frac{D_L}{R_a}\frac{\partial^2 C_f}{\partial x^2} + \frac{U_f}{R_a}\frac{\partial C_f}{\partial x} - \frac{2}{\delta}\frac{D_e}{R_a}\frac{\partial C_p}{\partial z}\bigg|_{z=0} = 0$$

$$0 \leq x \leq \infty \qquad (4.4.2)$$

The differential equation for the porous rock matrix can be written

$$\frac{\partial C_p}{\partial t} + \frac{\rho_p}{\varepsilon_p}\frac{\partial C_m}{\partial t} - \frac{D_e}{\varepsilon_p}\frac{\partial C_p}{\partial z^2} = 0$$

$$0 \leq z \leq \infty \qquad (4.4.3)$$

Assuming, for adsorption within the porous rock matrix, a linear equilibrium isotherm and introducing the matrix retardation factor R_d defined by the equation (4.1.7) the differential equation for the rock matrix becomes

$$\frac{\partial C_p}{\partial t} - \frac{D_e}{R_d \varepsilon_p}\frac{\partial^2 C_p}{\partial z^2} = 0 \qquad 0 \leq z \leq \infty \qquad (4.4.4)$$

The coupled system of equations (4.4.2) and (4.4.4) was solved by Tang et al. (1981) including radioactive decay for the following initial and boundary conditions:

$$C_f\ (0,\ t) = C_0 \qquad (4.4.5a)$$

$$C_f\ (\infty,\ t) = 0 \qquad (4.4.5b)$$

$$C_f\ (x,\ 0) = 0 \qquad (4.4.5c)$$

$$C_p\ (0,\ x,\ t) = C_f\ (x,\ t) \qquad (4.4.6a)$$

$$C_p\ (\infty,\ x,\ t) = 0 \qquad (4.4.6b)$$

$$C_p\ (z,\ x,\ 0) = 0 \qquad (4.4.6c)$$

where C_0 is the source concentration.

The concentration in the fracture may be written as

$$\frac{C(t)}{C_o} = \frac{2}{\sqrt{\pi}} \exp\left(\frac{Pe}{2}\right) \int_{\ell}^{\infty} \exp\left(-\xi^2 - \frac{Pe^2}{16\xi^2}\right) \cdot$$

$$\operatorname{erfc}\left(\frac{\frac{Pe\ t_o}{8\ A\ \xi^2}}{\sqrt{t - \frac{Pe\ t_o}{4\ \xi^2}}}\right) d\xi \qquad (4.4.7)$$

where

$$\ell = \left(\frac{Pe\ t_o}{4\ t}\right)^{1/2} \qquad (4.4.8)$$

$$Pe = \frac{U_f\ x}{D_L} \qquad (4.4.9)$$

$$t_o = R_a \frac{x}{U_f} = R_a\ t_w \qquad (4.4.10)$$

$$A = \frac{\delta\ R_a}{2\ (\varepsilon_p\ R_d\ D_e)^{1/2}} \qquad (4.4.11)$$

A similar model with a non-instantaneous reaction and slightly different boundary conditions was used on the same field data by Hodgkinson and Lever (1982).

4.5 Channeling dispersion-diffusion model

In the previous model the dispersion that occurs in the direction of the flow is accounted for by the hydrodynamic dispersion expressed as the Peclet number. This parameter takes into account the velocity variations in the fluid in a fissure, and the molecular diffusion. Another way to account for this dispersion is by means of channeling dispersion. The velocity differences in the channels will carry a tracer different distances over a given time. The tracer will be dispersed.

The transport of the tracers takes place through a fracture, in which parallel channels with different widths exist. A scheme of the flow conditions is shown in figure 3. It is assumed that the fissure widths show a lognormal distribution and the interconnection between the different channels is negligible. The hydrodynamic dispersion in each single channel is also assumed to be negligible compared to the effects of channeling.

The model includes the following mechanisms:

- o advective transport along the fissure
- o channeling dispersion
- o adsorption onto the surface of the channels
- o diffusion into the rock matrix
- o adsorption within the rock matrix.

Breakthrough curve for flow in a channel

For a tracer flowing through a fissure with negligible longitudinal dispersion, the equation for the concentration in the fissure is

$$R_a \frac{\partial C_f}{\partial t} + U_f \frac{\partial C_f}{\partial x} - D_e \frac{2}{\delta} \frac{\partial C_p}{\partial z}\bigg|_{z=0} = 0 \qquad 0 \leq x \leq \infty \qquad (4.5.1)$$

The equation for the diffusion into the rock is given by

$$\frac{\partial C_p}{\partial t} = D_a \frac{\partial^2 C_p}{\partial z^2} \qquad 0 \leq z \leq \infty \qquad (4.5.2)$$

where

$$D_a = \frac{D_e}{K_d \rho_p}$$

For a system which is initially free of tracer and where the concentration is suddenly increased to C_o at the inlet of the fissure (x=0), the initial and boundary conditions are

I.C. $C_f(x,0) = 0$ (4.5.3a)

$C_p(z,x,0) = 0$ (4.5.3b)

B.C. $C_f(0,t) = C_o$ (4.5.4a)

$C_p(0,x,t) = C_f(x,t)$ (4.5.4b)

$C_f(\infty,t) = 0$ (4.5.4c)

$C_p(\infty,x,t) = 0$ (4.5.4d)

The solution for the equations (4.5.1) and (4.5.2) with initial and boundary conditions (4.5.3) and (4.5.4) is found in the literature (Carslaw and Jaeger, 1959).

$$\frac{C_f}{C_o} = \operatorname{erfc}\left(\frac{D_e \, t_w}{\delta \, D_a^{1/2} \, (t-t_o)^{1/2}}\right) \qquad (4.5.5)$$

where $t_o = R_a \cdot t_w$

Breakthrough curve for the effluent

The fluid flows through various non-interconnecting channels in a fissure, with a channel width distribution $f(\delta)$. If the breakthrough curve for each channel is given as C_f (δ,t) then the concentration of the mixed effluent from all channels is (Neretnieks et al.,1982)

$$\frac{C(t)}{C_o} = \frac{\int_0^\infty f(\delta)\ Q(\delta)\ C_f(\delta,t)\ d\delta}{\int_0^\infty f(\delta)\ Q(\delta)\ d\delta} \qquad (4.5.6)$$

In a parallel-walled channel of width δ_i , the flow rate for laminar flow is proportional to the fissure width cubed

$$Q\ (\delta_i) = k_1\ \delta_i^3 \qquad (4.5.7)$$

The water residence time in a channel with width δ_i over a given distance is

$$t_{wi} = \frac{k_2}{\delta^2} = \bar{t}_w\ \left(\frac{\bar{\delta}}{\delta}\right)^2 \qquad (4.5.8)$$

The concentration at the outlet of a fissure with width δ_i, may be calculated introducing the equation (4.5.8) in equation (4.5.5), which becomes

$$\frac{C_f(\delta,t)}{C_o} = \text{erfc}\left(\frac{B\ \bar{t}_w\ \bar{\delta}^2}{\delta^3\ [t-\bar{t}_o(\ \bar{\delta}/\delta\ )^2\ ]^{1/2}}\right) \qquad (4.5.9)$$

where

$$B = \frac{D_e}{D_a^{1/2}} = (D_e\ K_d\ \rho_p)^{1/2} \qquad (4.5.10)$$

$$\bar{t}_o = R_a\ \bar{t}_w = \bar{t}_w(1 + \frac{2}{\delta}\ K_a) \qquad (4.5.11)$$

Fissure width distribution

Snow (1970) studied the fissure frequencies for various consolidated rocks including granites. He found that the fissure widths have a lognormal distribution. The density function has the form

$$f(\delta) = \frac{1}{\sigma \sqrt{2\pi}} \frac{1}{\delta} \exp \left(- \frac{[\ln(\delta/\mu)]^2}{2 \sigma^2} \right) \qquad (4.5.12)$$

where σ^2 is the variance of $\ln(\delta)$ and $\ln(\mu)$ is the mean of $\ln(\delta)$.

4.6 Hydrodynamic dispersion-diffusion and stagnant water model

It is assumed that the fluid flows through parallel channels in the same fissure, where the channels are separated by zones with stagnant fluid. The tracer migrates into the stagnant fluid in the fissure as well as into the rock matrix by molecular diffusion, and may be adsorbed onto the fissure surface and also penetrate the rock matrix adjacent to the fissure.

Only one channel is modelled. Several such identical channels are then coupled to act in parallel in a fissure. The individual channels do not influence each other. The tracer concentration across the width of the channel is assumed constant, due to the very low ratio of the width to the other dimensions of the channel. In the flow channel the concentration along the breadth of the channel is also set constant because computations including reasonable tranverse dispersion coefficients have shown this to be true. In the non-flow channels the transport is by molecular diffusion only and a concentration profile is developed.

The model includes the following processes:

- o Advective transport along the fissure
- o Axial hydrodynamic dispersion in the fracture
- o Molecular diffusion into the stagnant fluid in the fracture in the direction orthogonal to the flow
- o Diffusion into the rock matrix in the direction orthogonal to the fracture plane
- o Adsorption onto the surface of the fracture
- o Adsorption within the rock matrix.

Figure 4 shows the different processes in the channel.

The model is written for the linear flow of a tracer along a fisuure. The system is schematically defined in figure 4.

The differential equation for the tracer concentration in the flowing water in a channel in the fissure may be written as

$$\frac{\partial C_f}{\partial t} + \frac{2}{\delta}\frac{\partial C_s}{\partial t} + U_f \frac{\partial C_f}{\partial x} - D_L \frac{\partial^2 C_f}{\partial x^2}$$

$$-D_e \frac{2}{\delta}\frac{\partial C_p}{\partial z}\bigg|_{z=\frac{\delta}{2}} - D_w \frac{\delta'}{\delta}\frac{2}{\ell}\frac{\partial C_w}{\partial y}\bigg|_{y=\frac{\ell}{2}} = 0 \qquad (4.6.1)$$

The second term takes into account the adsorption onto the surface of the channel. The fifth term considers the diffusion into the rock matrix and the last one the diffusion into the stagnant water. δ' is the effective fissure width in the stagnant water zone and δ is the effective fissure width in the flowing water zone.

Assuming a linear equilibrium isotherm for the surface sorption and using the surface retardation coefficient equation (4.6.1) becomes

$$R_a \frac{\partial C_f}{\partial t} + U_f \frac{\partial C_f}{\partial x} - D_L \frac{\partial^2 C_f}{\partial x^2} - D_e \frac{2}{\delta}\frac{\partial C_p}{\partial z}\bigg|_{z=\frac{\delta}{2}}$$

$$- D_w \frac{\delta'}{\delta}\frac{2}{\ell}\frac{\partial C_w}{\partial y}\bigg|_{y=\frac{\ell}{2}} = 0 \qquad (4.6.2)$$

Neglecting diffusion in the x direction, the differential equation for the tracer concentration in the stagnant water is

$$\frac{\partial C_w}{\partial t} + \frac{2}{\delta'}\frac{\partial C_s}{\partial t} - D_w \frac{\partial^2 C_w}{\partial y^2} - D_e \frac{2}{\delta'}\frac{\partial C_p}{\partial z}\bigg|_{z=\frac{\delta'}{2}} = 0 \qquad (4.6.3)$$

A new surface retardation coefficient, R_a', is defined for the transport across the stagnant water. Then the equation (4.6.3) may be written as

$$R_a' \frac{\partial C_w}{\partial t} - D_w \frac{\partial^2 C_w}{\partial y^2} - D_e \frac{2}{\delta'} \frac{\partial C_p}{\partial z}\Big|_{z=\frac{\delta'}{2}} = 0 \qquad (4.6.4)$$

Finally, the differential equation for the porous rock matrix is

$$\frac{\partial C_p}{\partial t} + \frac{\rho_p}{\varepsilon_p} \frac{\partial C_m}{\partial t} - \frac{D_e}{\varepsilon_p} \frac{\partial C_p}{\partial z^2} = 0 \qquad (4.6.5)$$

Assuming a linear equilibrium isotherm for the adsorption within the porous rock matrix and introducing the matrix retardation coefficient R_d, the equation for the rock matrix becomes

$$R_d \frac{\partial C_p}{\partial t} - \frac{D_e}{\varepsilon_p} \frac{\partial C_p}{\partial z^2} = 0 \qquad (4.6.6)$$

5 FITTING OF EXPERIMENTAL DATA TO MODELS

5.1 The experimental data

The experimental measurements show an inadequate distribution. Most of the points are located on the flat part of the curves and very few points on the rising part. The fitted results are influenced by this distribution of the data because it overemphasizes one part of the curves. In the iodide tracer test, the distribution of the measurements along the time axis is:

- o at the rising part 9 measurements
- o at the flat part 83 "
- o at the descending part 33 "

If all the data are used in the fit, the calculations need a lot of computer time and the shape of the top has a greater influence on the results. A more even distribution may be obtained by using a weighting factor.

The computer time may be reduced by reducing the number of points used in the fit. In this case the experimental points first are smoothed. The concentration at a given time is obtained as the average value of the preceding. the actual and the following values. Then in the new data set only one point of three or four is included. If the number of points used in the fit is reduced by two-thirds, the same values are obtained for the parameters as when using all points. To de-emphasize the influence of the middle part a new data set is defined using the same number of points in each section of the experimental curve. In this last case the parameters show values different from the values obtained when all of the data points are used in the curve fit. These results are shown in table 5.1. The initial 120 points are reduced to about 40 points with a more even distribution. This data set is used in the calculations.

Table 5.1. Iodide tracer test. Reduction of the number of data points

	All of the data (or every third point)	15 points in each of rising, middle and descending parts
Pe	1.94	5.07
t_o, hr	51.7	39.1
$pf \cdot 10^3$	2.69	2.61

5.1 Parameter determination

In the preceding section the solution of the respective equations for a step function injection have been presented. The injection in the experiments was a rectangular pulse. For a finite rectangular pulse with duration Δt, the concentration at the outlet is obtained by subtracting the same function but delayed in time by Δt

$$C(L,t) = C_f(L,t) - C_f(L,t-\Delta t) \qquad (5.1.1)$$

The last term is zero for $t-\Delta t < 0$.

In the case of convergent radial flow, the calculation of the concentration in the pumping hole must include a proportionality factor. This factor considers the effect of the tracer dilution in the fissure and in the pumping well.

The parameter determination was done by means of a nonlinear least squares fitting using a routine from Nag-library.

The fitting process for each particular model is presented in appendix C.

The iodide tracer test is used for the determination of the hydraulic properties. These properties (i.e. Peclet number, water residence time, proportionality factor) are used in the strontium tracer test to predict breakthrough curves or determine sorption constants.

6.0 RESULTS

The tracer test for iodide was used to calculate the hydraulic properties of the flow path. The determination of the hydraulic properties includes:

- o water residence time
- o dispersion
- o proportionality factor.

The iodide is considered as a nonsorbing tracer ($K_d'=0$). Moreover the diffusion into the rock matrix is very low. For these reasons it is an adequate tracer for using in the determination of the hydraulic properties.

The strontium tracer test was used for testing the surface sorption constant determined in the laboratory. The volume sorption constant and the effective diffusivity into the rock matrix were tested as well, in the models that include the interaction with the matrix.

6.1 Results for the hydrodynamic dispersion in several pathways model

For the iodide tracer test this model was tested using one, two and three pathways. The results are shown in table 6.1. When one pathway is simulated the fitting is poor. With two or three pathways the agreement with the experimental data is much better. No big difference between two and three pathways was found. The fit for the three-pathway model is presented in figure 5.

Table 6.1. Three-pathway model. Iodide tracer test
Comparison with one and two pathways

	1-pathway model	2-pathway model	3-pathway model
Peclet number(1)	5.07	18.4	31.5
Residence time(1)	39.1	27.1	24.7
Proport. factor(1)	2.61	2.00	1.75
Peclet number(2)	-	18.4	31.5
Residence time(2)	-	114.	61.1
Proport. factor(2)	-	0.66	0.55
Peclet number(3)	-	-	31.5
Residence time(3)	-	-	153.
Proport. factor(3)	-	-	0.37
Standard deviation,%	7.2	4.3	3.8
Figure	-	-	5

In these calculations it is assumed that the Peclet number is equal in the different pathways. Table 6.2 presents the calculated hydraulic properties, for a three-pathway model. The tracer test for iodide was used to calculate the hydraulic properties of the fissures.

Table 6.2. Hydraulic properties of the fissures

Pathway	I	II	III
Flow rate ($Q \cdot 10^6$ m^3/s)	13.1	4.12	2.77
Hydraulic conductivity ($K_{pf} \cdot 10^3$ m/s)	4.76	1.92	0.77
Fissure width ($\delta_f \cdot 10^4$ m)	4.12	3.21	5.40
Equivalent fiss. width for laminar flow ($\delta_\ell \cdot 10^4$ m)	0.76	0.48	0.31
Water residence time (t_w hours)	24.7	61.1	153.
Peclet number	31.5	31.5	31.5

The strontium tracer test was studied using the three-pathway model. The hydraulic properties determined by the iodide tracer test were used in this case.

The surface sorption constant, K_a, was included in the parameter determination. A loss factor was also included due to the low recovery of strontium. A value of $7.2 \cdot 10^{-5}$ m was determined for the surface sorption coefficient on granite for the case of strontium (c.f. measured $7 \cdot 10^{-5}$ m, Skagius el al. 1982). The loss factor which is a measure of some unknown and not modelled interaction must be included to get a fair fit. The loss factor was 0.4 for the strontium run. The corresponding fit is shown in figure 6.

The solution for one-dimensional flow is a good approximation for the tracer transport in radial flow because in the actual runs the Peclet number was about 30.

Gustafsson and Klockars (1981) indicated that the tracers were diluted by a factor of 5 in the pumping hole, due to water flow from other levels. This value has been used in the calculations presented in this report. In the different runs the difference in hydraulic head has varied from 6.0 to 7.6 m with equal pumping rate. This would cause some variation of the flow rate through the fissures.

A model with 3 pathways can represent the tracer transport. Assuming that the Peclet number is equal in the different pathways, 7 parameters must be determined. The known effect of matrix diffusion is neglected however.

6.2 Results for the hydrodynamic dispersion-diffusion model

The results for the tracer test with iodide, with injection over 350 hours, are shown in table 6.3, first column. These results give too low a value for the parameter A if compared to available independent experimental data. The obtained A-value indicates too high an interaction with the rock matrix, corresponding to D_e equal to $1.8 \cdot 10^{-10}$ m^2/s, which is 3 orders of magnitude larger than the value obtained in experimental measurements in the laboratory (Skagius and Neretnieks, 1982).

From the water residence time obtained in this calculation the fissure width is calculated by means of equation (4.2.4), assuming that iodide is a nonsorbing tracer ($R_a = 1$).

The parameter A for iodide may be estimated using the value of D_e experimentally determined in the laboratory equal to $0.08 \cdot 10^{-12}$ m^2/s and the calculated value for the fissure width. In this case the value of A is about $3.0 \cdot 10^4$.

When a value of $3.0 \cdot 10^4$ is used for the parameter A the fit is poor. The concentrations at the top are constant and decrease rapidly to zero afterwards. The new values for the other parameters are also shown in table 6.3. In figure 7 the experimental value and the calculated curves for both cases are shown.

The results for the sorbing tracer test, strontium, when the fit includes the four parameters is shown in table 6.4, first column. The same value is obtained for Pe, but the proportionality factor is much smaller than the value from the iodide tracer test.

If the data for the proportionality factor and the Peclet number obtained from the iodide test are considered as known values and only the two parameters t_o and A for the strontium are fitted, a new set of values is obtained. These are shown in table 6.4, second column. The value obtained for the parameter t_o gives no physical meaning.

The values of the parameters t_o and A for strontium may also be calculated from the results of the iodide tracer test (Pe and pf) and other independent experimental measurements in the laboratory (Skagius et al., 1982). The predicted values are presented in table 6.4, fourth column. These values give too high an interaction with the matrix. Then the value for t_o is assumed to be correctly determined and the A-parameter is calculated by means of a fit. The new value for A is 320 and the corresponding curve is shown in figure 8. If $\varepsilon_p = 0.003$ and $K_d \cdot \rho_p = 20$, the value of the effective diffusion coefficient is $0.15 \cdot 10^{-12}$ m^2/s, while the value experimentally determined by Skagius et al. (1982) was $24.0 \cdot 10^{-12}$ m^2/s.

The concentration in the pumping hole was measured over 603 hours. In this time interval the recovery of the iodide reached about 100%, while the strontium recovery was only 62% for the same time interval. The recovery of the strontium calculated from the curve determined by a 4-parameter optimisation was 60 % in the first 603 hours. The recovery would reach a higher value if the time interval for integration was increased.

The proportionality factor may be directly determined from the experimental data. Results for the iodide ans strontium runs using this proportionality factor are shown in table 6.5. They are similar to the value obtained when the proportionality factor is included in the fit.

The results of the 4-parameter fit for the iodide run show a very small value for the parameter A, indicating an important interaction between the matrix and the tracer. This does not agree with experimental measurements in the laboratory. The iodide is considere as a nonsorbing substance ($R_a = 1$) and the effective diffusivity D_e has a value of $0.08 \cdot 10^{-12}$ m^2/s.

This difference can be explained by other mechanisms not included in the model, for example:

i) The tracers flow through various pathways from the injectio hole to the pumping hole, with different residence times in each pathway.

ii) The tracers diffuse into alteration materials coating the fissure surface with much higher sorption capacity, porosit or diffusivity, or a combination of the three

When the parameter A is calculated from experimental measurements in the laboratory and this value is used in a three-parameter fit, the Peclet number obtained in the curve fit is smaller.The Peclet number in this case includes the effects of hydrodynamic dispersion as well as other dispersive mechanisms not included in the model.

Table 6.3 Iodide tracer test.

	4-parameter optimisation	3-parameter optimisation, $A = 3 \cdot 10^4$ ([1])
Pe	86.9	5.24
t_0 hrs	18.3	38.5
A	320	$3.0 \cdot 10^4$
$pf \cdot 10^3$	2.99	2.62
s	0.04	0.07
$D_e \cdot 10^{12}$ m^2/s	180.	0.08
δ, mm	0.466	0.981
Figure	7	7

([1]) Parameter A calculated from experimental determinations in the laboratory.

Table 6.4. Strontium tracer test

	4-parameter optimisation	2-parameter optimisation([1])	1-parameter optimisation([2])	Predicted values([3])
Pe	73.1	5.24	5.24	5.24
t_θ hr	18.0	4.80	43.9	43.9
A	210	25.5	320.0	25.5
$pf \cdot 10^3$	1.94	2.62	2.62	2.62
$D_e^* \cdot 10^{12}$ m^2/s	0.35	24.0	0.15	24.0
s	0.04	0.07	0.12	
Figure	-	-	8	8

([1]) Pe and pf obtained from the iodide tracer test when the parameter was equal to $3.0 \cdot 10^4$.

([2]) Pe and pf determined as in ([1]) and t_0 calculated from experimental measurements in the laboratory.

([3]) Pe, pf and t_0 determined as in ([2]) and A calculated from experimental measurements in the laboratory.

(-) underlined values = given values.

* D_e as such is not fitted. It is obtanied from "A" by using laboratory data on ε_p and R_d and is given only for comparison.

Table 6.5. Results obtained with proportionality factor calculated as injection rate/pumping rate

	Iodide run 3-parameter optimisation	Iodide run 2-parameter optimisation([1])	Strontium run 1-parameter optimisation([2])	Strontium run predicted values([3])
Pe	19.1	4.73	4.73	4.73
t_o	24.9	39.8	45.4	45.4
A	754	$3.0 \cdot 10^4$	300	26.6
$pf \cdot 10^3$	2.7	2.7	2.7	2.7
s	0.06	0.07	0.12	

([1]) parameter A calculated from determinations in the laboratory.

([2]) Pe obtained from the iodide run with A equal to $3.0 \cdot 10^4$ and t_o calculated from measurements in the laboratory.

([3]) Pe and t_o as in ([2]) and A calculated from experimental measurements in the laboratory.

(-) underlined values = given values.

6.3 Results for the channeling dispersion-diffusion model

First a fit is done for the nonorbing tracer, iodide, including the four parameters (σ, B, t_w and pf). The results show a B-parameter corresponding to a D_e value of $1.75 \cdot 10^{-10}$ m^2/s. This value does not agree with experimental measurements in the laboratory (Skagius and Neretnieks, 1982).If the B-parameter is calculated using the value of D_e determined in the laboratory ($0.08 \cdot 10^{-12}$ m^2/s) and the fit is done for the other three parameters, the agreement is poor. The concentration at the top is constant and decreases rapidly to zero afterwards. The values for both cases are shown in table 6.6; and the corresponding curves are shown in figure 9.

Similar results were obtained when the iodide test was evaluated using the hydrodynamic dispersion-diffusion model. These values are shown in table 6.7.

For the sorbing tracer, strontium, a fit including the four parameters shows a proportionality factor which is only 60 % of the value corresponding to the iodide run. This means that there is an unaccounted loss of 40 %.

The channeling dispersion, the water residence time and the dilution effect are equal in both runs because they are determined by the hydraulic conditions of the system. So, the values of σ, t_w and pf obtained from the iodide run may be used, and the other two parameters (K_a and B) may be calculated by means of a fit. The results in this case give a value of about zero for the surface adsorption equilibrium constant. For this reason the value of K_a experimentally determined in the laboratory (Skagius et al., 1982) is included and then the fit is only done for the B-parameter. The results show a value of B corresponding to a D_e value of $0.20 \cdot 10^{-12}$ m^2/s, which is about 2 orders of magnitude less than the D_e value of $24.0 \cdot 10^{-12}$ m^2/s determined in the laboratory.

In table 6.8 the results for the two fits are shown, together with the parameters of the curve predicted using values of the iodide run (σ, t_w, pf) and values experimentally determined in the laboratory (K_a, K_d, D_e). The corresponding curves are shown in figure 10. Similar results are obtained in the respective fits when this run is evaluated with the hydrodynamic dispersion-diffusion model.

Table 6.6. Iodide tracer test

	4-parameter optimisation	3-parameter optimisation B = $1.55 \cdot 10^{-8}$ ([1])
σ	0.072	0.285
B	$7.24 \cdot 10^{-7}$	$\underline{1.55 \cdot 10^{-8}}$
t_w, hrs	18.8	41.4
pf$\cdot 10^3$	2.98	2.61
s	0.04	0.07
$D_e \cdot 10^{12}$ m^2/s	175	0.08
δ, mm	0.479	1.06
Figure	9	9

([1]) Parameter B calculated from experimental determinations in the laboratory.

(-) underlined values = given values.

Table 6.7. Comparison with the hydrodynamic dispersion-diffusion model. Iodide run.

	Channeling dispersion model	Hydrodynamic dispersion model
4-parameter fit		
t_w, hrs	18.8	18.4
δ, mm	0.479	0.468
$D_e \cdot 10^{12}$ m^2/s	175	180
3-parameter fit ($D_e=0.08 \cdot 10^{-12}$ m^2/s)		
t_w, hrs	38.6	38.4
δ, mm	1.06	0.978

Table 6.8. Strontium tracer test

	2-parameter optimisation([1])	1-parameter optimisation([2])	Predicted values([3])
σ	0.285	0.285	0.285
B	$2.26 \cdot 10^{-6}$	$2.20 \cdot 10^{-6}$	$2.19 \cdot 10^{-5}$
t_w, hrs	41.4	41.4	41.4
$pf \cdot 10^3$	2.61	2.61	2.61
K_a, m	$< 1.0 \cdot 10^{-14}$	$7 \cdot 10^{-5}$	$7 \cdot 10^{-5}$
s	0.08	0.09	
$D_e \cdot 10^{12}$ m^2/s	0.26	0.24	24.0
Figure	-	10	10

([1]) σ, t_w and pf obtained from the iodide tracer, when the experimental D_e value for iodide was used ($D_e = 0.08 \cdot 10^{-12}$ m^2/s).

([2]) σ, t_w and pf as in ([1]) and using the experimental value of K_a ($K_a = 7 \cdot 10^{-5}$ m).

([3]) σ, t_w, pf and K_a as in ([2]) and B was calculated using the experimental D_e value ($D_e = 24 \cdot 10^{-12}$ m^2/s).

(-) underlined values = given values.

6.4 Results for the hydrodynamic dispersion-diffusion and stagnant water model

For the nonsorbing tracer test with iodide, the values used in the different runs and results are shown in table 6.9. When channels of 1.0 m in breadth are simulated the results do not agree well with the experimental results. The concentration is constant at the top and the calculated values do not explain the tail observed in the experimental data. The diffusion into the stagnant water is not significant due to the low ratio between the area for diffusion and the channel volume.

As the channel breadth is reduced, the number of channels and their widths have to be increased to obtain flow sections sufficiently large for the total flow through the fissure. A better agreement is obtained when a smaller channel breadth is used in the simulations. A small channel breadth must be compensated by a large width to obtain the same residence time. The smallest channel breadth used is 0.10 m. This corresponds to a channel width about 2.5-3.0 mm.

In the runs with small channel breadth, the effect of the diffusion into the rock is decreased primarily because the exposed surface is smaller. The diffusion into the stagnant water becomes more significant at the same time. The runs 1-3 with channel breadths of 1.0, 0.20 and 0.10 m respectively are presented in figure 11. In all the cases the Peclet number is 40. For this value of the dispersion the calculated values agree very well with the rising part of the experimental curve, but the agreement is bad at the top and in the tail of the curve. The influence of the Peclet number is shown in figure 12. The data in the run 3 are used except for the Peclet number. For a Peclet number of 10 a better global agreement is obtained, but in this case the adjusted curve shows a greater dispersion in the rising part.

For the sorbing tracer test, strontium, the calculations were done using the same channel size and the same hydraulic properties as in the runs for the iodide test. The values experimentally determined by Skagius et al. (1982) were used for K_a, K_d and D_e. They give a greater interaction between the tracer and the rock matrix than the experimental data. The value of D_e that gives the best fit is about one order of magnitude less than the value experimentally determined in the laboratory. In the next run, the breakthrough curve is calculated using a D_e value of $2.4 \cdot 10^{-12}$. In this case a rather good agreement with the experimental data is obtained, the results being shown in figure 13.

The model used here assumes channeling and stagnant water volumes in the fissure. Strong channeling has been observed in real fissures (Neretnieks et al.,1982 and Abelin et al.,1982). It also seems reasonable to assume that more or less stagnant volumes may exist. The above analysis has shown that this type of model has the capability of giving a reasonable fit to the experimental data using channel breadths well in accordance with field observations. The channel widths needed in this model seem to be too large however.

Table 6.9. Non-sorbing tracer test, Iodide.
Parameters used in the simulations.

	Run 1	Run 2	Run 3	Run 4
ℓ, m	1.00	0.20	0.10	0.10
$\delta \cdot 10^3$ m	0.88	1.54	2.42	2.92
ε_f	1.0	1.0	1.0	1.0
Pe	40	40	40	10
t_w, h	27	25	25	30
$D_w \cdot 10^9$ m^2/s	2.0	2.0	2.0	2.0
$D_e \cdot 10^{12}$ m^2/s (1)	0.08	0.08	0.08	0.08
ρ_f	0.0026	0.0027	0.0027	0.0028
Figure	11/12	11	11	12

(1) Value determined in the laboratory by Skagius and Neretnieks (1982)

7.0. DISCUSSION

The simplest model used here is the hydrodynamic dispersion in several pathways model with only surface sorption. This model neglects diffusion into the rock matrix and there is no a priori way of choosing the number of channels or the properties of the channels.

Two and three pathways give very similar results for the iodide run and a prediction of the strontium data using only surface sorption data would be good if a 40 % tracer loss could be accounted for. As the model neglects the known effect of matrix diffusion and sorption within the rock matrix and 5 to 7 independent entities must be determined to describe the hydraulic situation it is not deemed to be a useful model for prediction. It can, however, be used to fit the data very well.

The next three models all include matrix diffusion. The model with hydrodynamic dispersion in a single channel and the model with a multitude of independent channels are very similar in that only one entity determines the flow dispersion effects. In the first case it is the dispersion coefficient D_L and in the second it is the standard deviation of the fissure width distribution.

Although the models give very similar results when fitted to the experimental data the models describe different physical spreading mechanisms. The impact of channeling on the prediction of radionuclide migration when data from short distance experiments are used to predict migration over large distances has been shown to be severe in some circumstances (Neretnieks 1981). It is therefore interesting to note that these two spreading mechanisms cannot be distinguished from the present experimental data. Tracer tests along the same pathway but with observations at different distances would be helpful in discriminating between the two mechanisms.

In the presentation of the results for the case of the iodide run, the values determined by Skagius and Neretnieks (1982) for the effective diffusivity in Finnsjö granite of the iodide have been used. This value is $0.08 \cdot 10^{-12}$ m^2/s. In another recent report by the same authors (1983) values in the range $0.09\text{-}2.50 \cdot 10^{-12}$ m^2/s are given for the effective diffusivity of the iodide in pieces of granite with coating material. The porosity values were as large as 0.019 for granite with coating material.

In the hydrodynamic dispersion-diffusion model an A-value of $3.0 \cdot 10^4$ was used to fit the experimental data. If values of $2.5 \cdot 10^{-12}$ m^2/s for the effective diffusion and 0.015 for the porosity are assumed a new value of A is obtained. As this new value is used in the fit (A = 2000) the agreement is better than with a value of $3.0 \cdot 10^4$. The results of this fit are shown in table 7.1 and figure 14.

To predict the breakthrough curve for strontium, the values determined for crushed granite by Skagius et al. (1982) were used. Values of effective diffusion coefficient and volume equilibrium constant determined for sawed pieces of granite are also shown in table 2.1. If the latter values are used to calculate the A-parameter a value of about 120 is obtained instead of 25.5. The difference between the fitted "best" value of A = 267 (Table 7.1 column 2) and A = 120 has decreased considerably. In this case there is still an unaccounted loss of 40 % of the strontium. The predicted curve is shown in figure 15 (curve 1).

In the calculation of the strontium tracer run it was assumed that the relationship between the concentration in the liquid phase and the tracer concentration sorbed on the solid phase is linear. Using this assumption the surface retardation factor and the volume retardation factor were defined. The values determined for volume equilibrium constant by Skagius et al. (1982) were obtained working with concentrations below 10-15 mg/l.

In the actual field experiments the concentration in the injection hole was about 8000 mg/l. Because of this, a check was recently made on the sorption of strontium at higher concentrations (Skagius,1983). For concentrations above 20 mg/l the isotherm is not linear. It is described by a Freundlich isotherm $C_m \propto C_p^n$ with n=0.41. The differential equations are then nonlinear and they would be solved by means of numerical methods.

An approximate solution may be obtained through the linearisation of the isotherm at the actual concentration. If we consider that the tracers are diluted by the axial and tranverse dispersion, a reasonable value of about 2000 mg/l may be assumed to calculate the new equilibrium constant. Assuming that the Freundlich exponent is equal for surface and volume sorption isotherms, the calculations for this concentration would be done using a value of $3.6 \cdot 10^{-6}$ m for the surface equilibrium constant and a value of 0.38 m^3/ton for the sorption within the rock matrix. If the A parameter is calculated using these values and keeping $D_e = 2.20 \cdot 10^{-12}$ m^2/s a value of 273 is obtained, while the value determined in the fit is 223. The results of the fit are shown in table 7.1, column 3 and figure 15 (curve 2). As D_e contains a high proportion of surface diffusion it will change with concentration and the comparison is thus somewhat oversimplified.

The model which includes stagnant zones of water gives a better agreement for the iodide without adjusting the matrix diffusion parameters, because a similar affect as matrix diffusion is obtained by letting the iodide diffuse into the stagnant water. For the sorbing tracer strontium on the other hand, the available surface from which diffuses into the rock matrix has been reduced considerably. The strontium does not diffuse at all as far into the stagnant water because it is retarded by sorption and matrix diffusion. Thus the effective sorption surface decreases compared to the case with flow in all the fissure. Although there probably are stagnant zones of water, in reality the model needs so many adjustable parameters that it is at present not suited for prediction purposes.

Table 7.1

Parameter for iodide and strontium fits
for new values determined in the laboratory.

Tracer	I([1])	Sr([2])	Sr([3])
Pe	8.1	8.1	8.1
t_o,hrs	32.3	37.8	32.6
A-parameter,fitted	-	267.	223.
A-parameter,calculated	2000.	120.	273.
D_e*$\cdot 10^{12}$ m^2/s	2.50	2.20	2.20
pf$\cdot 10^3$	2.7	2.7	2.7
s	0.06	0.13	0.12
δ, mm	0.82	0.82	0.82

([1]) Parameter A calculated from experimental measurements in the laboratory. Values determined in sawed pieces of granite.

([2]) Pe and pf obtained from the iodide tracer test in ([1]) and t_o calculated from experimental measurements in the laboratory.

([3]) Pe and pf obtained as in ([2]) and t_o calculated considering the isotherm for the strontium to be nonlinear.

(-) underlined values = given values.

* Value of D_e used for calculating the A-parameter.

8.0 CONCLUSIONS

Various interacting mechanisms of a sorbing and a nonsorbing tracer have been tested.

Attempts to fit experimental data to the four models have shown that a single channel model with hydrodynamic dispersion as the sole spreading mechanism is not sufficient to fit the experimental data. A multichannel model gives a reasonable fit but neglects the known interactive mechanism of matrix diffusion.

The hydrodynamic dispersion model and the model which includes fissure width distribution as a cause for dispersion give good fits with four adjustable parameters. The parameter which accounts for interaction with the matrix indicates that the nonsorbing tracer has a much higher interaction than laboratory data on granite indicate. Recent measurements on fissure-coating materials show that porous coatings exist which may give sufficiently large interaction to account for the observed interaction. This applies for both models.

It has not been possible to distinguish between hydrodynamic dispersion and dispersion caused by differences in fissure width. To do this experiments at different distances are necessary.

The sorbing tracer test indicates that the interaction with the matrix is much weaker than can be explained by diffusion and sorption in granite only if sorption data for low concentrations are used. The concentration in the field experiment was probably two orders of magnitude higher than the original laboratory data. A recent measurement at high concentration indicates that the sorption coefficient decreases considerably at high concentrations. The indications are that this is the major cause for the discrepancy.

The attempt to use a model with diffusion into stagnant zones of water in addition to matrix interaction and hydrodynamic dispersion, is inconclusive because 2 more adjustable parameters are used and the effect of the stagnant water is small if reasonable geometries are chosen.

NOTATION

a	specific surface	m^2/m^3 fluid
A	parameter defined in eq. 4.4.11	
B	parameter defined in eq. 4.5.10	
C_f	concentration in the liquid in the fissure	mol/m^3
C_m	concentration in the solid	mol/kg
C_p	concentration in the liquid in the pores	mol/m^3
C_s	concentration on the surface of the solid	mol/m^2
C_w	concentration in the stagnant water	mol/m^3
D_a	apparent diffusivity	m^2/s
D_e	effective diffusivity into the rock	m^2/s
D_L	dispersion coefficient	m^2/s
D_w	molecular diffusion coefficient in water	m^2/s
h	hydraulic head	m
K_a	surface equilibrium constant	m
K_d	volume equilibrium constant	m^3/kg
K_{pf}	hydraulic conductivity of fissure	m/s
pf	proportionality factor	
Pe	Peclet number	-
Q	flow rate	m^3/s
r	radial distance	m
R_a	surface retardation factor in the channel	
R'_a	surface retardation factor in the stagnant water	
R_b	matrix retardation factor	
s	relative standard deviation in the fit	
t	time	s
t_o	tracer residence time	s
t_w	water residence time	s
U_f	water velocity	m/s

x	distance in the direction of flow	m
y	distance into stagnant water	m
z	distance into rock matrix	m
δ	fissure width in the channel in the fissure	m
δ'	fissure width in the stagnant water zone	m
ε_f	ratio δ'/δ	
ε_p	porosity of rock matrix	
ℓ	channel breadth	m
ℓ	parameter defined in equation 4.4.12	
μ	parameter in the lognormal distribution	
ρ_p	density of rock matrix	kg/m^3
σ	standard deviation in the lognormal distribution	
υ	kinematic viscosity	m^2/s

REFERENCES

Abelin, H., Gidlund, J. and Neretnieks, I.: "Migration in a single fissure", Proceeding of the Material Research Society Fifth International Symposium. Berlin, June 1982, West Germany.

Abramowitz, M. and Stegun, I.A.: "Handbook of Mathematical Functions". Dover publications, New York (1972)

Allar, B.; Kipatsi, H. and Torstenfelt, B.:"Adsorption of long lived radionuclides in clay and rock". KBS TR 98, Nuclear Fuel Safety Project, Stockholm (1978).

Bear, J.: "Hydrodynamic dispersion. Flow through porous media". (R.J.M. de Wiest ed.) Academic Press, New York (1969).

Carslaw, H.S. and Jaeger, J.C.: "Conduction of heat in solids", 2nd ed., Oxford University Press, New York (1959).

Edwards, A.L.: "TRUMP: A computer program for transient and steady-state temperature distribution in multidimensional systems." Lawrence Livermore Laboratory, California, U.S.A.(1972)

Gustafsson, E. and Klockars, C.E.: "Studies on groundwater transport in fractured crystalline rock under controlled conditions using non-radioactive tracers". KBS TR 81-07, Nuclear Fuel Safety Project, Stockholm (1981).

Hodkinson, D.P. and Lever, D.A.: Interpretation of a field experiment on the transport of sorbed and non-sorbed tracers through a fracture in crystalline rock. AERE-R-10702, Harwell, Nov. 1982.

Landström, O.; Klockars, C.E.; Holmberg, K.E. and Westerberg, S.: "In situ experiments on nuclide migration in fractured crystalline rocks". KBS 110, Nuclear Fuel Safety Project, Stockholm (1978).

Landström, O.; Klockars, C.E.; Persson, O.; Andersson, K.; Torstenfelt, B.; Allard, B.; Tullborg, E.L. and Larsson, S.A.: "Migration experiments in Studsvik" KBS 83-yy, Nuclear Fuel Safety Project, Stockholm (1983).

Lenda, A. and Zuber, A.: "Tracer dispersion in ground water experiments" Proceedings of a symposium organized by IAEA, Vienna (1970).

Neretnieks, I.:" Diffusion in the Rock Matrix: An Important Factor in Radionuclides Retardation? ". J. of Geophysical Res., Vol 85, 4379 (1980).

Neretnieks, I.: "Prediction of radionuclide migration in the geosphere. - Is the porous flow model adequate?" IAEA Symposium on migration in the terrestrial environment of long-lived radionuclides from the nuclear fuel cycle. Knowville Tennessee USA, 27-31 July 1981.

Neretnieks, I.; Eriksen, T. and Tähtinen, P.: "Tracer Movement in a Single Fissure in Granitic Rock: Some Experimental Results and Their Interpretation", Water Resources Res., Vol 18, 849 (1982).

Ogata, A and Banks, R.: "A solution of the Differential Equation of Longitudinal Dispersion in Porous Media". US Geological Survey Prof. Paper 411-A, Washington (1961).

Sauty, J.P.: "An analysis of hydrodispersive transfer in aquifers", Water Resources Res., Vol 16, 145-58 (1980).

Skagius, K. and Neretnieks, I.: "Diffusion in crystalline rocks of some sorbing and nonsorbing species." KBS TR 82-12, Nuclear Fuel Safety Project, Stockholm (1982).

Skagius, K. and Neretnieks, I.: "Diffusion Measurements in crystalline rocks". KBS TR 83-15, Nuclear Fuel Safety Project, Stockholm (1983).

Skagius, K.; Svedberg, G. and Neretnieks, I.: "A study of strontium and cesium sorption on granite". Nuclear Technology, Vol 59, 332 (1982).

Skagius, K., Dept. Chem. Eng., Royal Inst. Technology, Stockholm, personal comm., April 1983.

Snow, D.T.: "The frequency and apertures of fractures in rock", Int. J. Rock. Mech. Min. Sci., vol. 7, 23 (1970).

Tang, G.H.; Frind, E.O. and Sudicky, E.A.: "Contaminant Transport in Fractured Porous Media. An Analytical Solution for a Single Fracture" Water Resources Res., Vol 17, 555 (1981).

APPENDIX A

Experimental data.

Tracer test with simultaneus injection during 350 h of Iodide and Strontium; time after injection and concentration

Time (h)	C/C_o Sr^{2+} $\cdot 10^3$	C/C_o I^- $\cdot 10^3$	Time (h)	C/C_o Sr^{2+} $\cdot 10^3$	C/C_o I^- $\cdot 10^3$
16		0.03	122	1.36	2.48
18		0.13	126	1.37	2.35
20		0.38	130	1.40	2.33
22	0.14	0.62	134	1.35	2.35
24		0.95	138	1.41	2.34
26	0.34	0.07	142	1.34	2.30
28		1.35	146	1.35	2.34
30	leaking valve		150	1.37	2.36
32		1.55	154	1.40	2.41
34	0.66	1.58	158	1.43	2.47
38	0.78	1.70	162	1.43	2.49
42	0.84	1.76	166	1.41	2.41
46	0.92	1.79	170	1.38	2.42
50	0.93	1.80	174	1.41	2.45
54	0.95	1.79	178	1.43	2.45
58	0.95	1.78	182	1.42	2.51
62	0.98	1.83	184	1.43	2.56
66	0.99	1.88	188	1.47	2.65
70	1.04	1.89	192	1.41	2.74
74	1.08	1.93	196	1.52	2.77
76		2.14	200	1.58	2.83
78	leaking valve		204	1.60	3.05
80		2.16	208	1.65	3.05
82	1.16	2.04	212	1.65	2.92
86	1.18	2.07	216	1.57	2.85
90	1.22	2.12	220	1.57	2.76
94	1.24	2.16	224	1.53	2.68
98	1.28	2.21	228	1.49	2.68
102	1.31	2.27	234	1.58	2.68
106	1.34	2.27	238	1.52	2.60
110	1.34	2.26	242	1.54	2.60
114	1.35	2.24	246	1.53	2.53
116		2.35	250	1.49	2.52
118	1.35	2.45	254	1.48	2.56

Cont.

Time (h)	C/C_o Sr^{2+} $\cdot 10^3$	C/C_o I^- $\cdot 10^3$	Time (h)	C/C_o Sr^{2+} $\cdot 10^3$	C/C_o I^- $\cdot 10^3$
258	1.44	2.26	423	0.39	0.41
262	1.44	2.61	426	0.39	0.36
266	1.48	2.66	434	0.35	0.29
270	1.47	2.67	442	0.32	0.26
274	1.52	2.71	450	0.30	0.14
278	1.48	2.77	458	0.26	0.22
282	1.54	2.74	466	0.24	0.19
286	1.59	2.77	474	0.25	0.18
290	1.61	2.80	482	leaking valve	
294	1.63	2.82	490	0.22	0.16
298	1.65	2.83	499	0.23	0.15
302	1.71	2.88	507	0.18	0.13
306	1.71	2.91	515	0.17	0.12
310	1.71	2.88	522	0.17	0.11
314	1.72	2.89	530	0.16	0.12
318	1.86	2.86	538	0.14	0.11
322	1.92	2.86	546	0.17	0.09
326	1.93	2.89	554	0.14	0.09
328	1.95	2.89	562	0.14	0.09
332	1.82	2.71	570	0.13	0.07
336	1.83	2.73	578	0.07	0.06
340	1.88	2.80	586	0.01	0.04
344	1.63	2.82	595	0.07	0.01
348	1.64	2.88	603	0.01	0.04
352	1.65	2.90			
357	1.66	2.92			
363	1.64	2.71			
369	1.64	2.11			
375	1.20	1.66			
381	1.00	1.27			
387	0.86	1.03			
393	0.71	0.83			
399	0.61	0.68			
405	0.55	0.59			
411	0.49	0.51			
417	0.45	0.45			

APPENDIX B

Extension of dispersion-diffusion model to two pathways

The case of a fluid carring tracers through two pathways is considered. Like the case with one pathway, the model includes dispersion in each pathway, diffusion into the rock matrix, adsorption onto the surface of the fissure and adsorption within the rock matrix.

The concentration at the outlet of each pathway is given by the equation (4.4.7) in this report. The resulting concentration of the two pathways may be expressed as

$$C = \sum_{1}^{2} C\,(Pe_i,\ t_{wi},\ A_i,\ pf_i) \qquad (B.1)$$

The fit of this relationship to the experimental data requires the determination of eight parameters. The number of parameters to determine may be reduced by:

- o assuming that the Peclet numbers in both pathways are equal. If the dispersion coefficient is assumed to be directly proportional to the velocity, then the Peclet number is only a function of the distance and of the dispersivity. The dispersivity may be regarded as a medium property

$$Pe = Pe_1 = Pe_2 \qquad (B.2)$$

- o calculating the total proportionality factor from the experimental conditions. In this case the ratio of the injection rate to the pumping rate is $2.7 \cdot 10^{-3}$

$$pf_1 + pf_2 = pf_t = 2.7 \cdot 10^{-3} \qquad (B.3)$$

- o estimating the A-parameters for the non-sorbing tracer, iodide, from experimental measurements in the laboratory.

In this manner, the parameters which must be determined in the fit are reduced to four for a non-sorbing tracer

$$C_f = f(Pe, t_{w1}, t_{w2}, pf_1) \qquad (B.4)$$

For the sorbing tracer, strontium, the Peclet number, the water residence times and the proportionality factors calculated from the iodide tracer run will be used. The fit for the strontium is reduced to only two parameters (K_a and D_e). The value of $K_d \cdot \rho_p$ is assumed to be known.

Results

Two cases were studied. The first one considers that the fluid flows through two fissures with different widths but with the same breadth. In the second case it is assumed that both pathways exist in one fissure, each pathway being a fraction of the flow section. The difference between the cases is that in the first case there is twice as much exposed surface for sorption as in the second case.

For the non-sorbing tracer, iodide, the value of De determined in the laboratory ($0.08 \cdot 10^{-12}$ m^2/s) was used in the fit in both cases. For the strontium tracer run the values to determine are K_a and D_e. When the fit included these parameters, the results gave no physical meaning, as a value of less than 1.0 was obtained for R_a. For this reason the value of D_e only was included in the fit, while K_a was calculated from measurements in the laboratory and the fissure widths previously calculated.

The results are shown in tables B.1-2 and figures B.1-2. For flow through two fissures a D_e value equal to $0.044 \cdot 10^{-12}$ m^2/s was obtained. The value determined in the laboratory is $24.0 \cdot 10^{-12}$. For flow through one fissure the value of D_e is greater ($0.24 \cdot 10^{-12}$), but is still 2 orders of magnitude less than the value experimentally determined.

Table B.1 Results for the two pathway model.
Flow through two fissures.

Iodide

	Path 1	Path 2
Peclet number	18.0	18.0
A-parameter$\cdot 10^{-4}$	1.7	2.3
Water resid. time, hr	27.0	118.
Rel. prop. factor	0.76	0.24
Fissure width, mm	0.52	0.72

Strontium

Surface retard. factor	1.27	1.19
A-parameter	355.	458.
Effective difusivity $D_e \cdot 10^{12}$ m^2/s	0.044	0.044

Table B.2 Results for the two pathway model.
Flow through one fissure.

Iodide

	Path 1	Path 2
Peclet number	17.7	17.7
A-parameter$\cdot 10^{-4}$	4.0	4.0
Water resid. time, hr	27.0	118.
Rel. prop. factor	0.76	0.24
Fissure width, mm	1.26	1.26

Strontium

Surface retard. factor	1.11	1.11
A-parameter	320.	320.
Effective difusivity $D_e \cdot 10^{12}$ m^2/s	0.24	0.24

APPENDIX C

C.1 Hydrodynamic dispersion-diffusion model

The relative tracer concentration at the outlet of each fissure is a function of two parameters (Pe and t_R). If it is assumed that the tracer transport occurs through 3 pathways, the total concentration is calculated by

$$C_f = \sum_{1}^{3} pf_i \cdot C\ (Pe_i,\ t_{Ri}) \qquad (C.1.1)$$

The proportionality factor takes into account the dilution effect and the tracer distribution between the three fissures.

The hydraulic properties determined from the iodide tracer test are used for the Strontium test. The surface sorption constant is included in the parameter determination. Due to the low recovery of strontium a loss factor was also included in the fitting process.

C.2 Hydrodynamic dispersion-diffusion model

Evaluation of the integral

The integral in equation (4.4.7) has no analytical solution and is evaluated numerically. To improve the integration new narrower limits are chosen. The maximum absolute error accepted in the evaluation of the integrand is defined as

$$\varepsilon = \frac{1.0\ 10^{-6}}{\exp\left(\frac{Pe}{2}\right)} \qquad (C.2.1)$$

To determine the lower limit, ξ is calculated considering that the exponential function or the erfc function in the integrand is equal to ε. The greater of these two values is the lower limit of the integral

$$\xi_i^2 = \text{Max} \begin{cases} -\frac{\ln\varepsilon}{2}\left(1 - \sqrt{1 - \frac{Pe^2}{4\,(\ln\varepsilon)^2}}\right) \\ \\ \frac{\ell^2}{2}\left(1 + \sqrt{1 - \frac{t}{A^2\,\ln\varepsilon}}\right) \end{cases} \qquad (C.2.2)$$

In the second case the Asymptotic solution for erfc is used (Abramowitz and Stegun, 1970).

The upper limit is calculated considering that the value of the exponential function is less than 1.0. The upper limit of the integral is

$$\xi_f^2 = -\frac{\ln\varepsilon}{2}\left(1 + \sqrt{1 - \frac{Pe^2}{4\,(\ln\varepsilon)^2}}\right) \qquad (C.2.3)$$

The numerical integration was done by means of Gaussian quadrature (NAG-routine D01BDF). Typically 30-50 points were used to obtain a relative accuracy of 0.1 %.

Determination of the Parameters

The concentration in the pumping hole may be written as

$$\frac{C_f}{C_o} = pf\ f_2(\ Pe,\ t_o,\ A,\ t,\ \Delta t) \qquad (C.2.4)$$

where pf is the proportionality factor, which is determined from the mass of injected tracer, the injection time and pumping rate as

$$pf = \frac{m}{r_p\ \Delta t\ C_o} \qquad (C.2.5)$$

In general, it is necessary to determine 3 parameters: Pe, t_o and A. Δt and pf are generally known from the experimental conditions. This last parameter, pf, is not necessarily determined with any accuracy. Also in the model unaccounted losses may occur e.g. by some of the tracer moving into fluid which does not arrive at the pumping hole. For this reason the proportionality factor is included in the fit.

C.3 Channeling dispersion-diffusion model

The concentration at the outlet of a fissure with width δ_i, may be calculated introducing the equation (4.5.8) in equation (4.5.5), which becomes

$$\frac{C_f(\delta,t)}{C_o} = \text{erfc}\left(\frac{B\ \bar{t}_w\ \bar{\delta}^2}{\delta^3\ [t-\bar{t}_w(\ \bar{\delta}/\delta\ )^2\ ]^{1/2}} \right) \qquad (C.3.1)$$

where

$$B = \frac{D_e}{D_a^{1/2}}$$

Then the concentration resulting from all fissures may be expressed as

$$\frac{C_f(t)}{C_o} = f\ (\ \mu,\ \sigma,\ B,\ \bar{t}_w,\ t\ ) \qquad (C.3.2)$$

The value of μ in the equation (4.5.10) is determined so that the set of channels with varying widths has the same flow rate as if all channels had equal width, $\bar{\delta}$. The ratio $\mu/\bar{\delta}$ is a function of σ only.

The value of $\bar{\delta}$ is determined from the mean residence time as

$$\bar{\delta}^3 = \int_0^\infty f(\delta)\ \delta^3\ d\delta \qquad (C.3.3)$$

C.4 Hydrodynamic dispersion-diffusion and stagnant water model

In the field experiment the flow is radial. Here the flow is represented by a linear flow through a fissure of length L and breadth W. L is the distance from the injection hole to the pumping hole and W is the circumference of a circle centred on the pumping hole, with radius equal to L/2.

The fissure width in the channels is calculated considering the total flow Q through the fissure and the water residence time t_w

$$\delta = \frac{Q\ t_w}{L\ \ell\ n} \qquad (C.4.1)$$

where ℓ is the channel breadth and n is the number of channels that may exist in the fissure.

For a nonsorbing tracer test, the following parameters must be determined:

- o Peclet number
- o water residence time
- o coefficient of molecular diffusion into the stagnant water
- o coefficient of effective diffusion into the rock
- o proportionality factor, which takes into account dilution effect
- o channel breadth
- o channel width
- o number of channels
- o ratio δ'/δ.

Of these only the diffusivities have been determined by independent measurements. The other parameters are obtained by comparing the experiment with model results. The equations are numerically solved

using the computer program TRUMP (Edwards, 1972). No optimisation is carried out, breakthrough curves are only determined for certain values of the parameters. The effective diffusion coefficient in granite determined experimentally in the laboratory by Skagius and Neretnieks (1982) is used. The calculations are done using a value of 1.0 for the ratio δ'/δ.

The channel geometry and the number of channels required are determined by considering the area available to the flow and the distance between channels. This distance should be great enough to allow the tracer to diffuse a fair distance into the stagnant water, but small enough to allow the tracer to reach the furthest point (from the channels).

For the case of the strontium test, the equilibrium constants K_a and K_d must be included in the study. The channel size and hydraulic properties used in the iodide run are used for the strontium run.

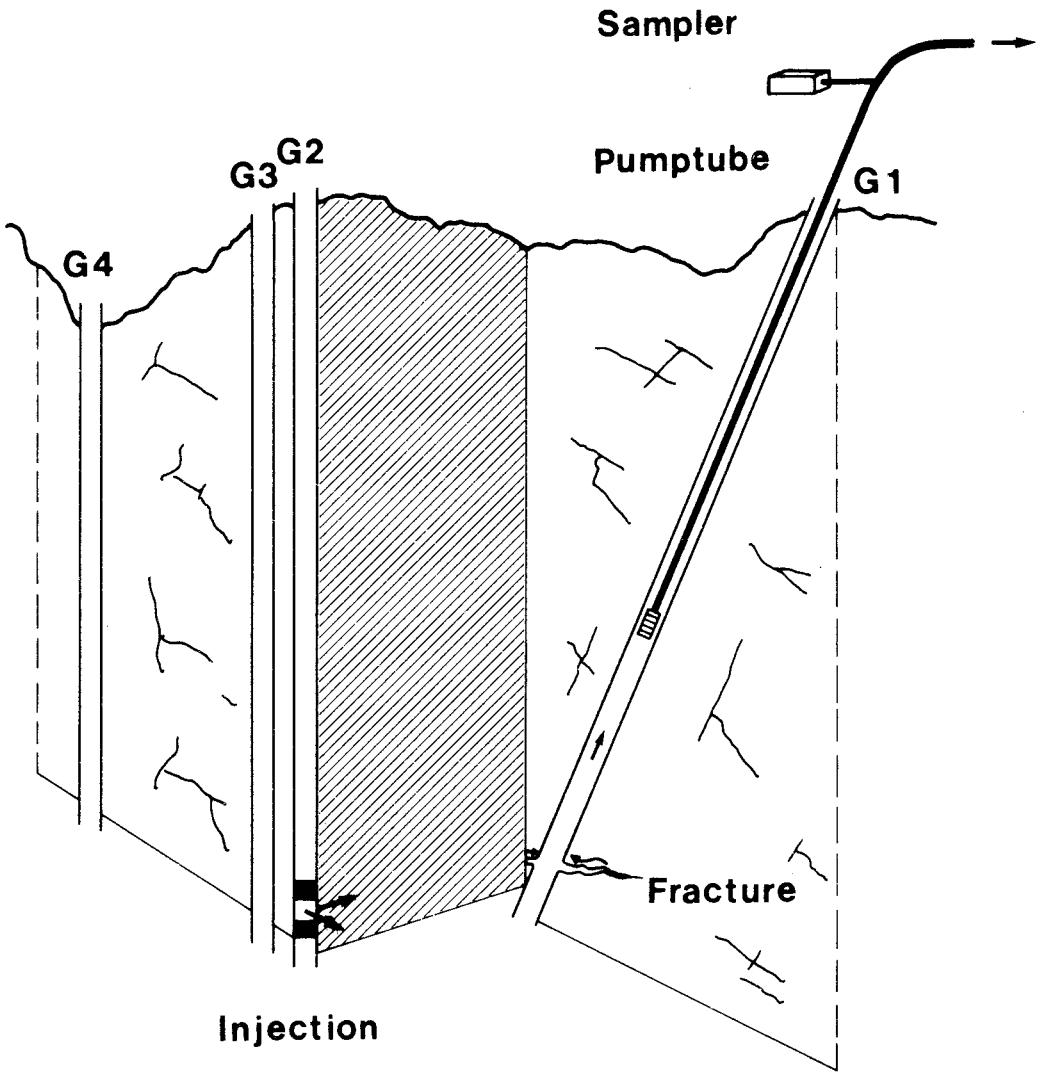

Figure 1.- Cutaway view of test site and apparatus set-up.

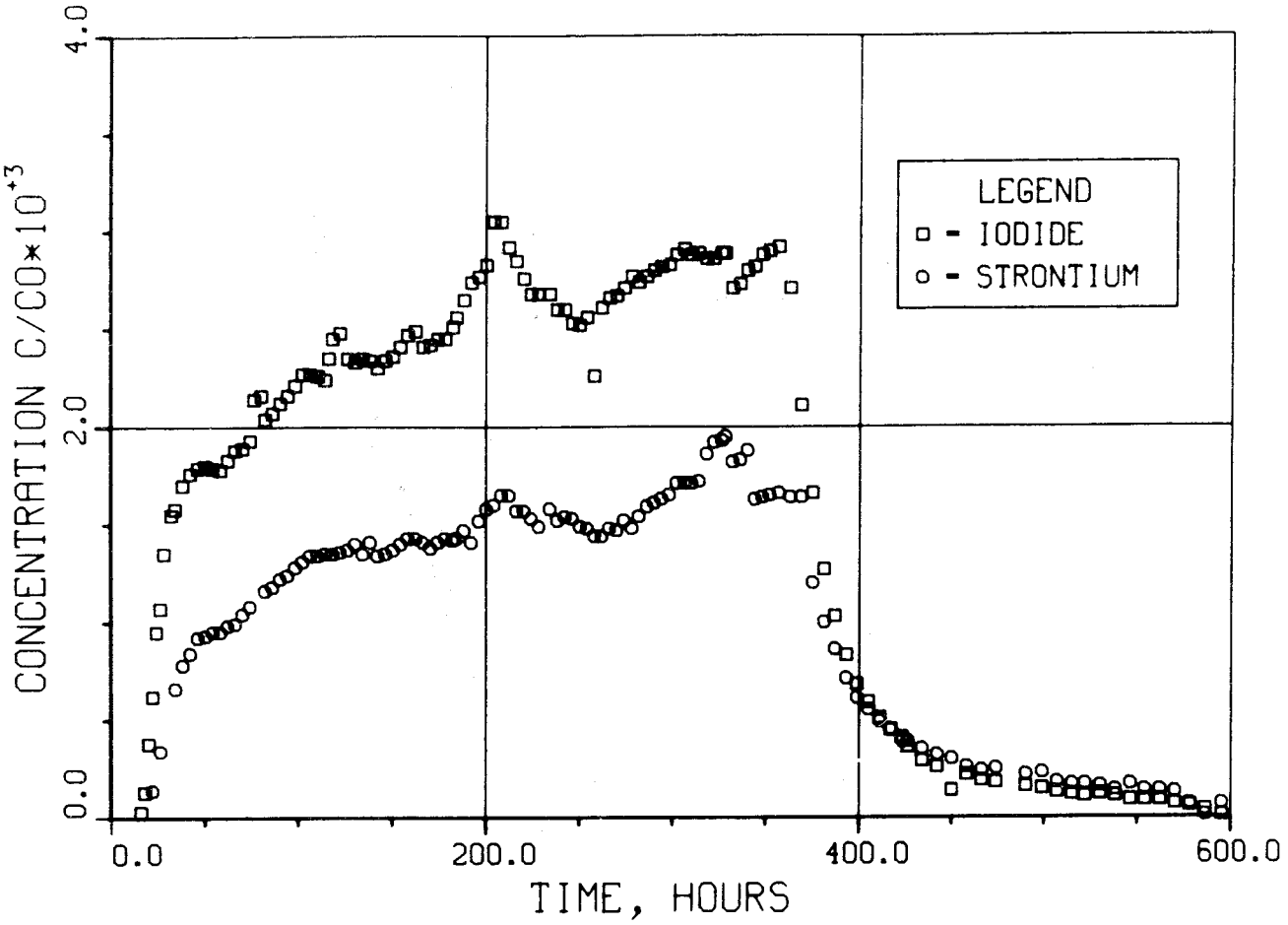

Figure 2.- Experimental breakthrough curves for iodide and strontium. (Data from appendix A.)

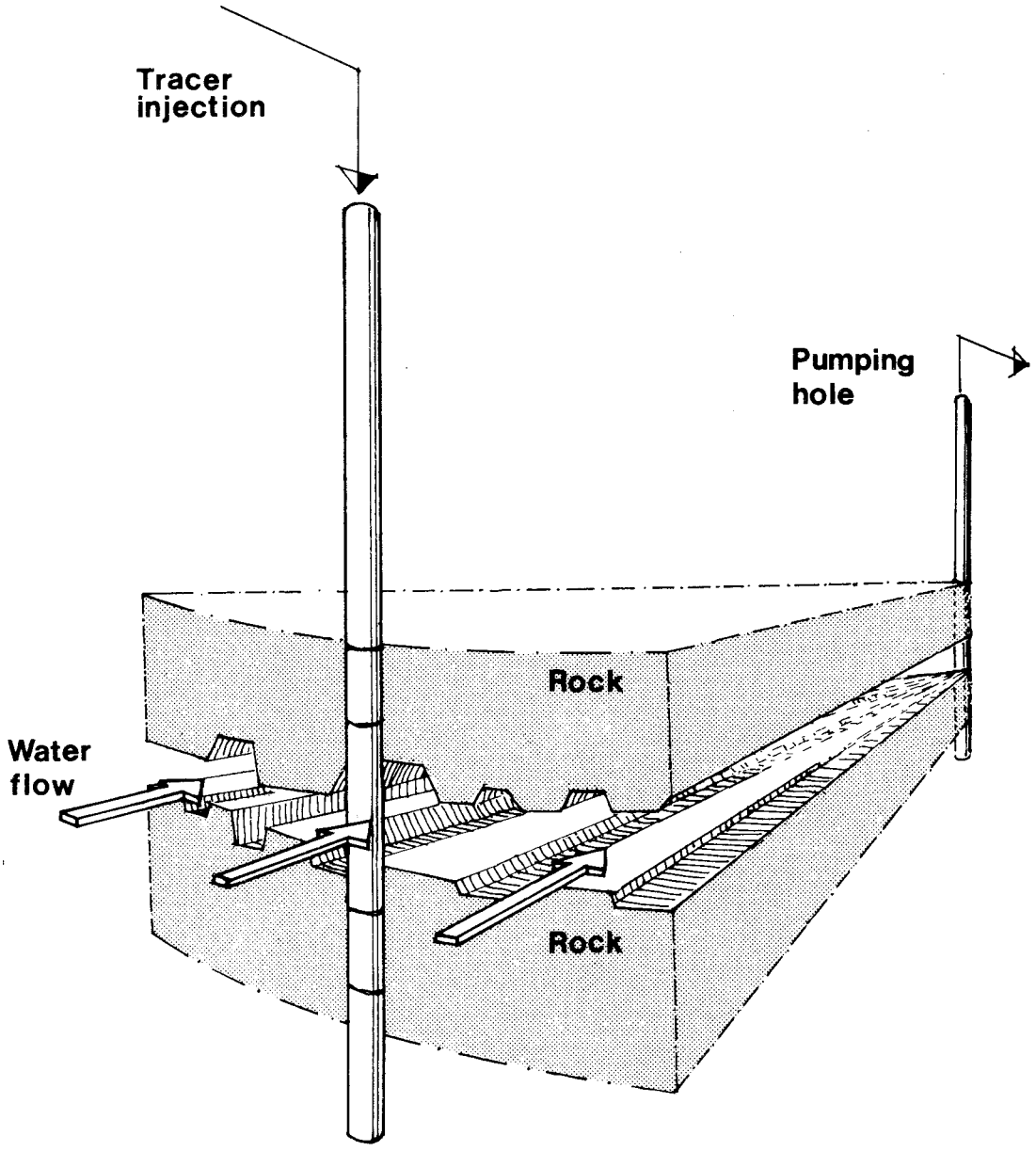

Figure 3.- Scheme for the channeling dispersion-diffusion model.

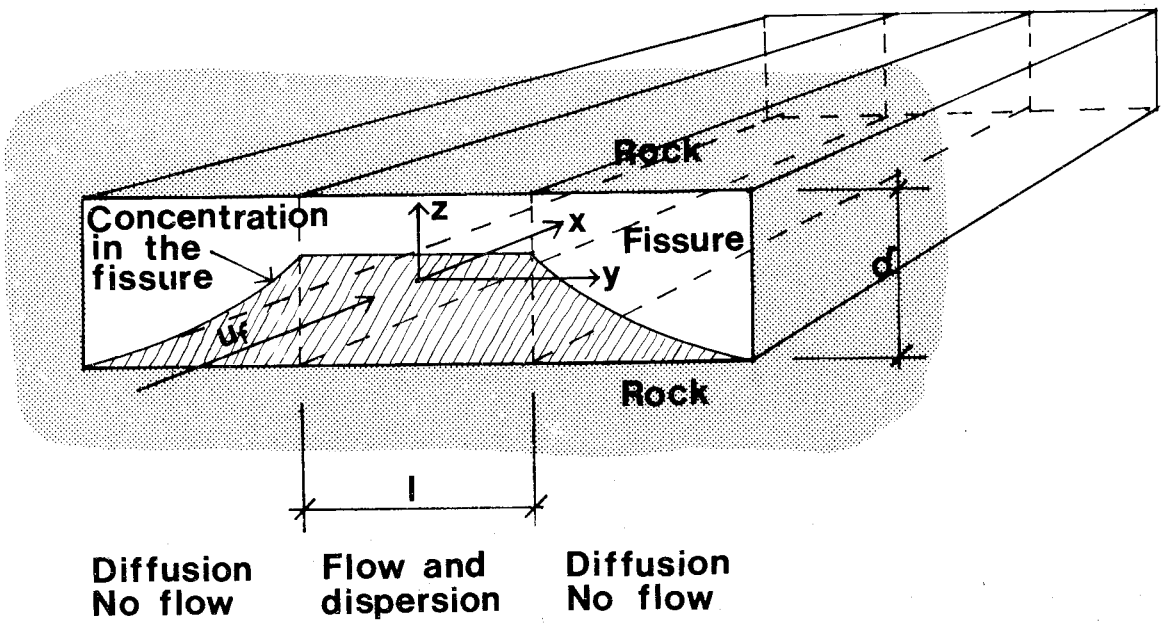

Figure 4.- Scheme for the hydrodynamic dispersion-diffusion and stagnant water model.

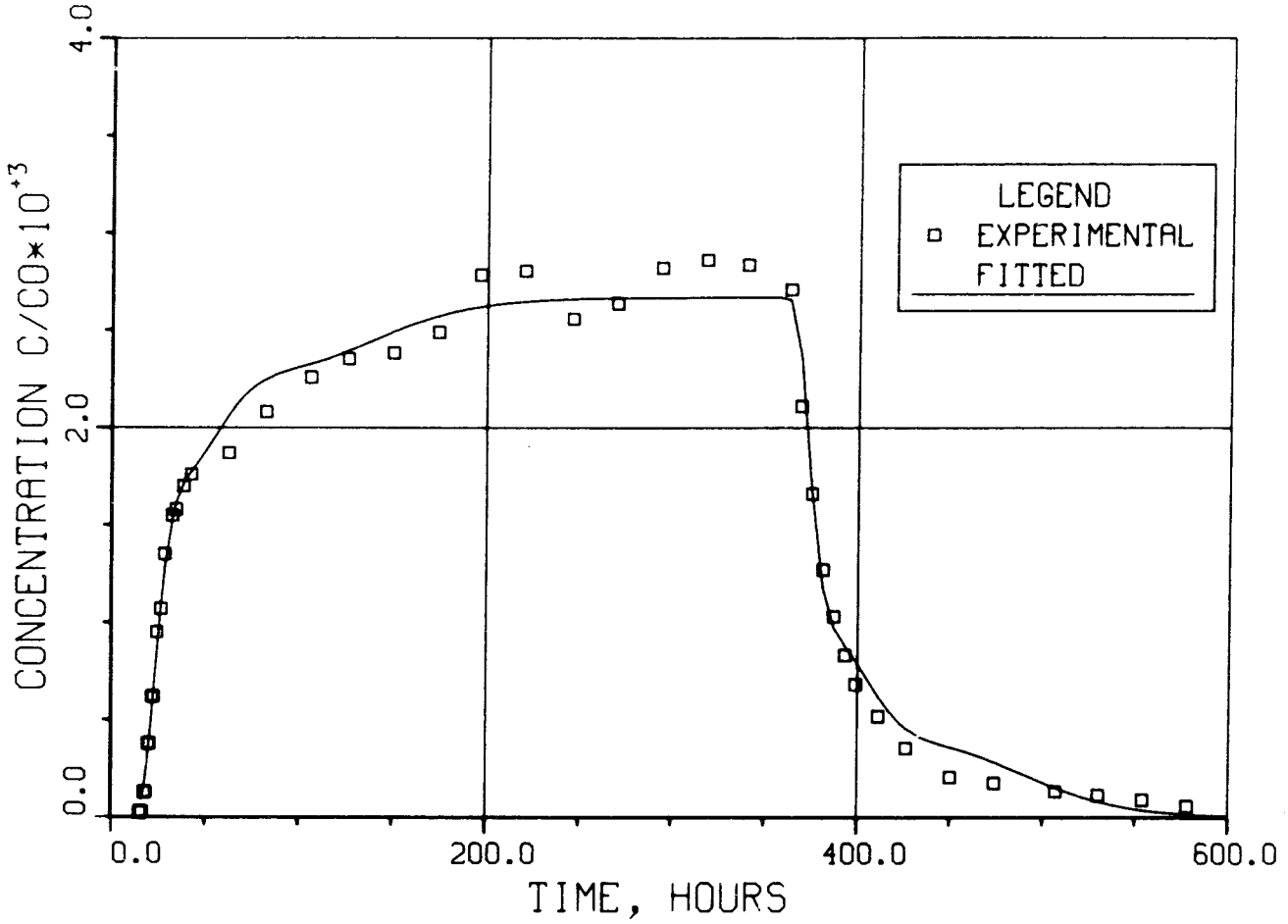

Figure 5.- Experimental data for iodide and fit using the hydrodynamic dispersion in three pathways model (Table 6.1, column 3).

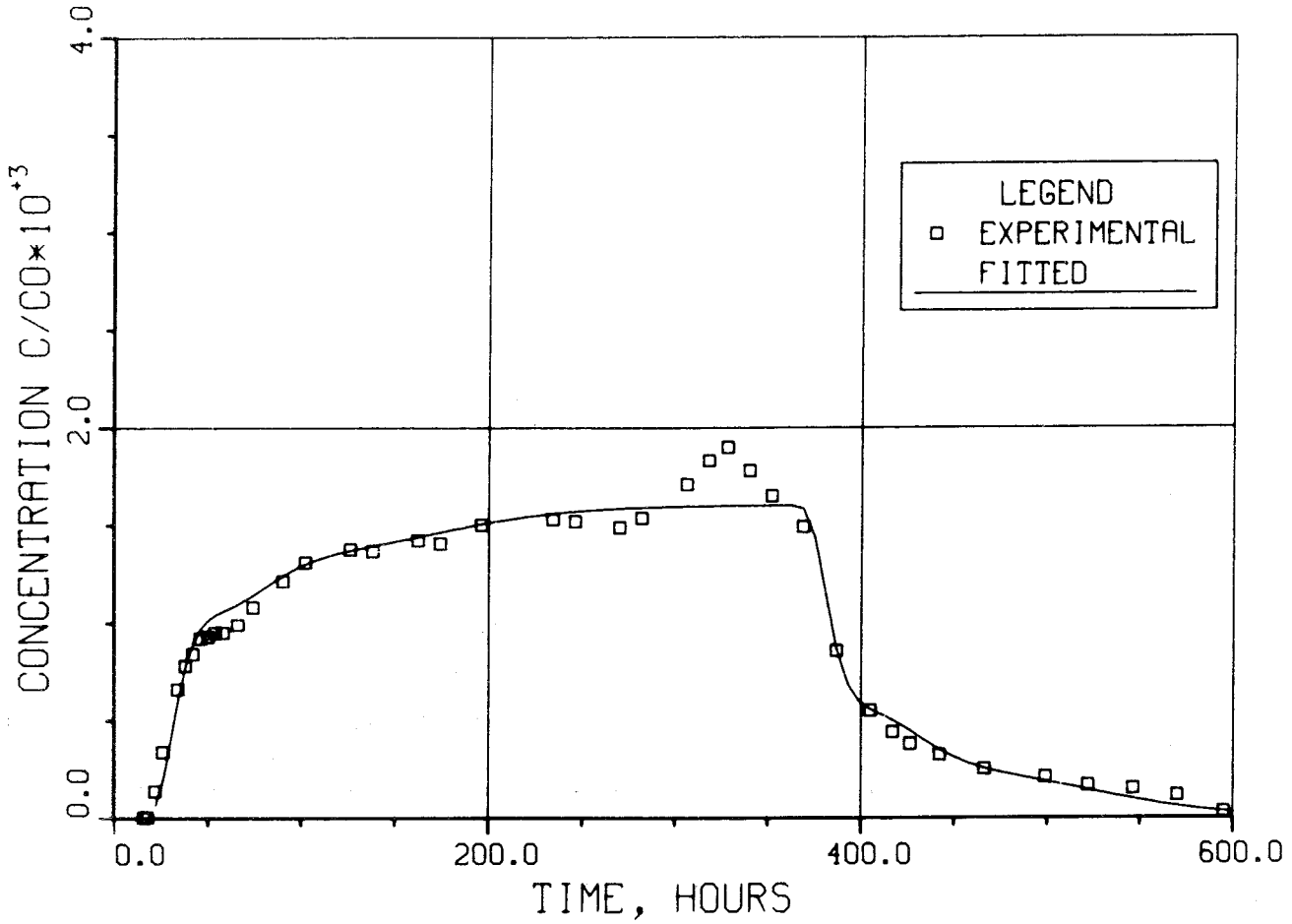

Figure 6.- Experimental data for strontium and fit using the hydrodynamic dispersion in three pathways model.

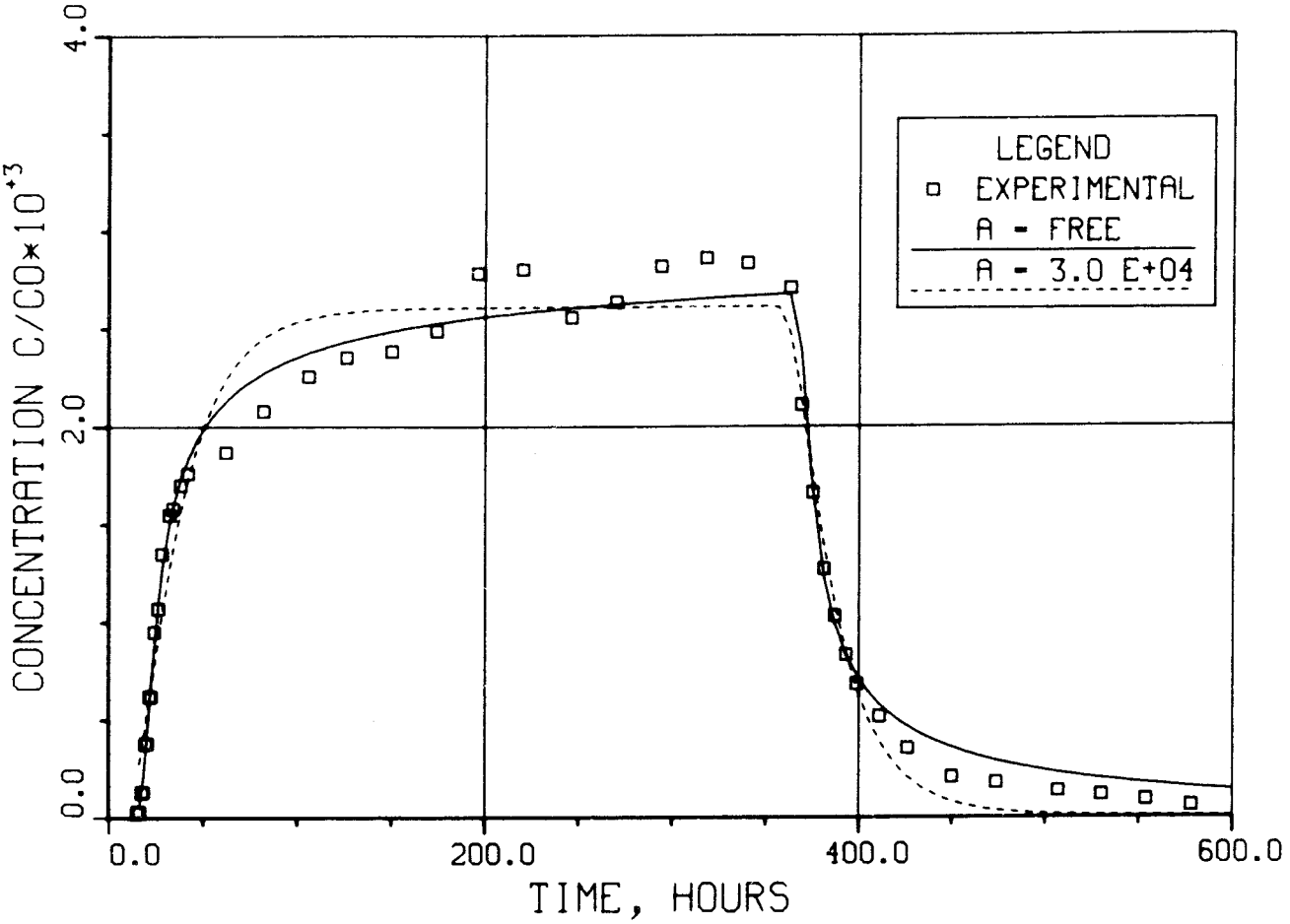

Figure 7.- Experimental data for iodide and curves calculated using the hydrodynamic dispersion-diffusion model, with the A-parameter determined by a fit (Table 6.3, column 1) and the A-parameter determined from experimental measurements in the laboratory (Table 6.3, column 2).

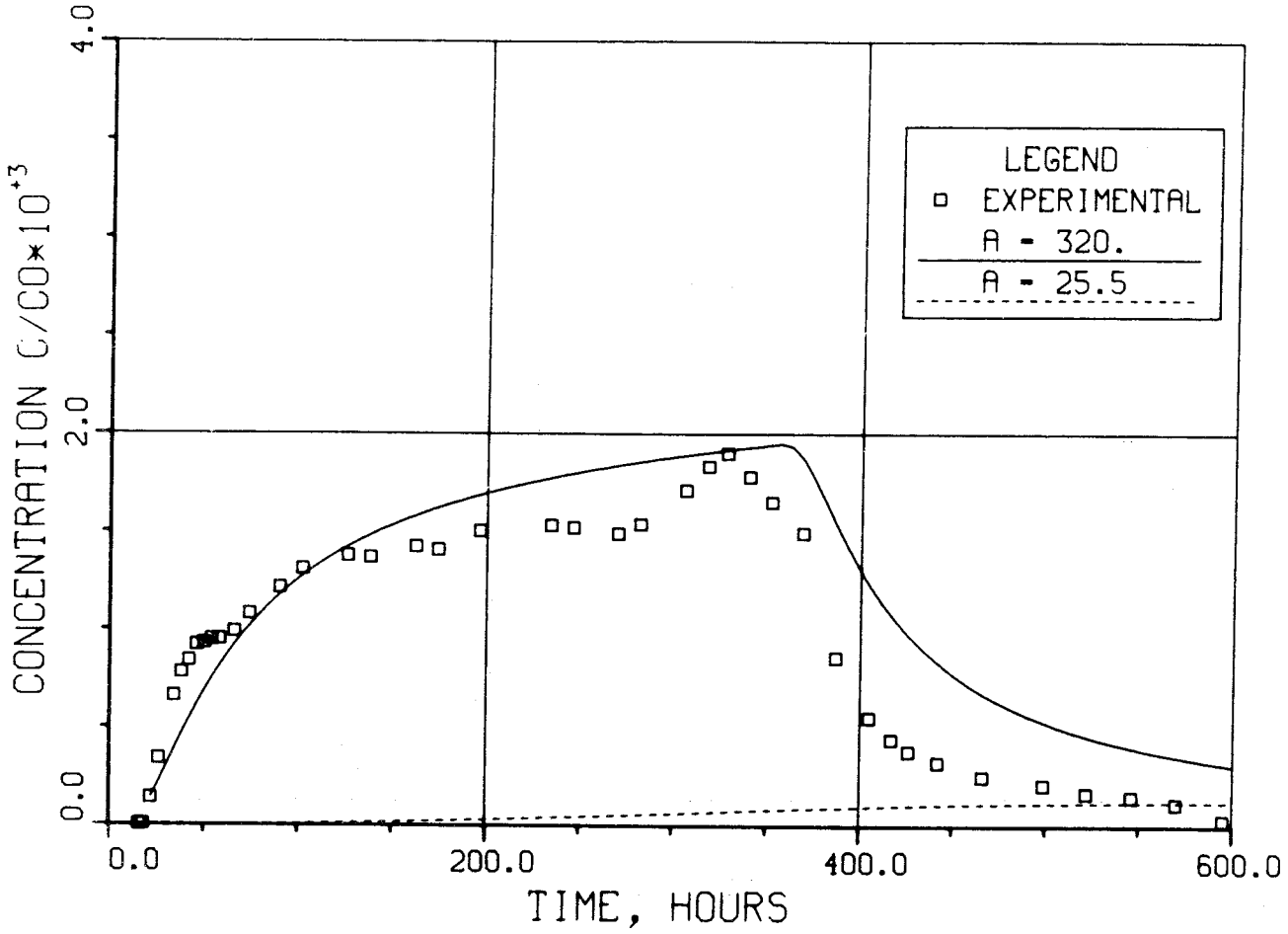

Figure 8.- Experimental data for strontium and curves calculated using the hydrodynamic dispersion-diffusion model, with the A-parameter determined by a fit (Table 6.4, column 3) and the A-parameter determined from experimental measurements in the laboratory (Table 6.4, column 4).

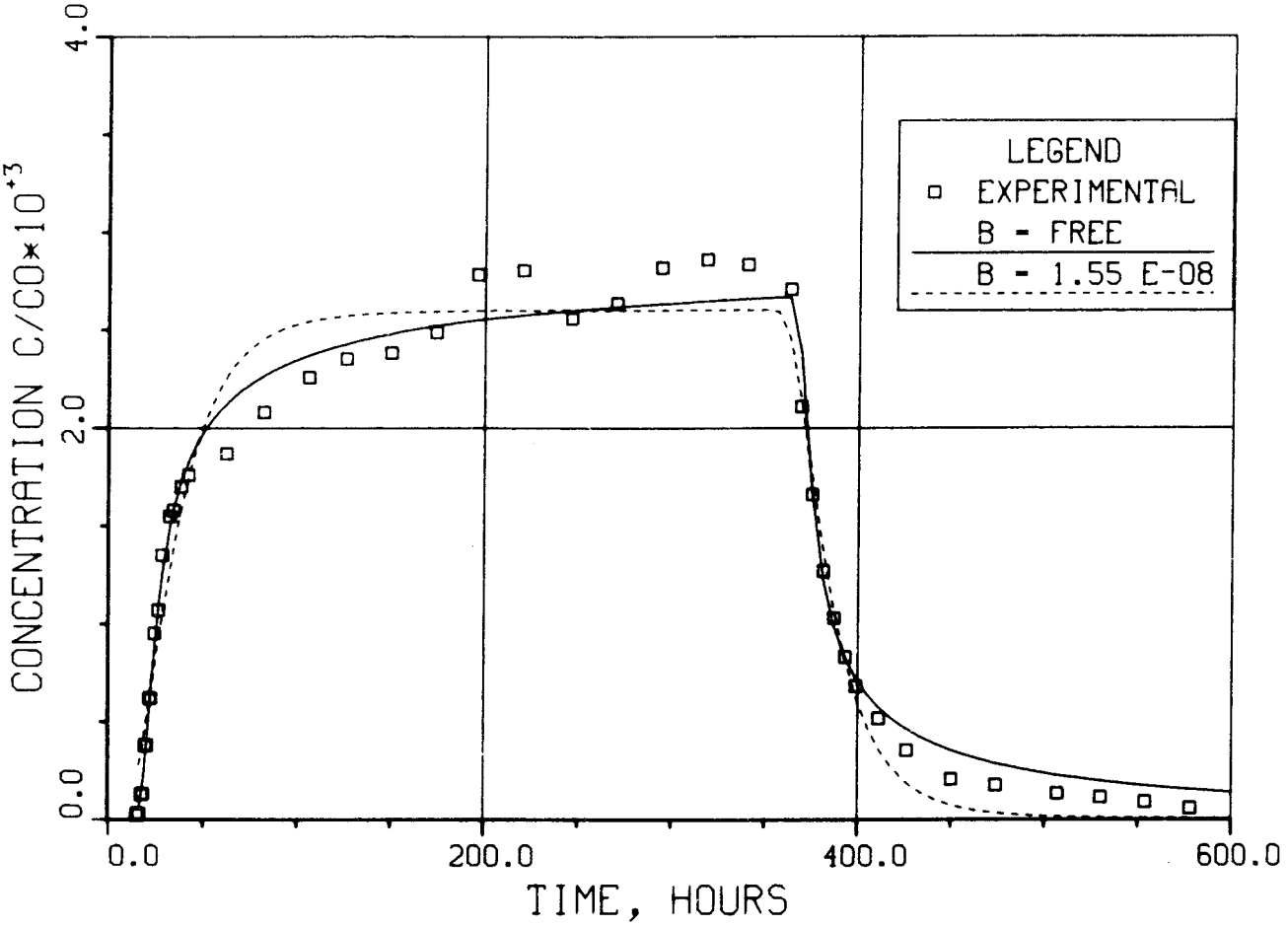

Figure 9.- Experimental data for iodide and curves calculated using the channeling dispersion-diffusion model, with the B-parameter determined by a fit (Table 6.6, column 1) and the B-parameter determined from experimental measurements in the laboratory (Table 6.6, column 2).

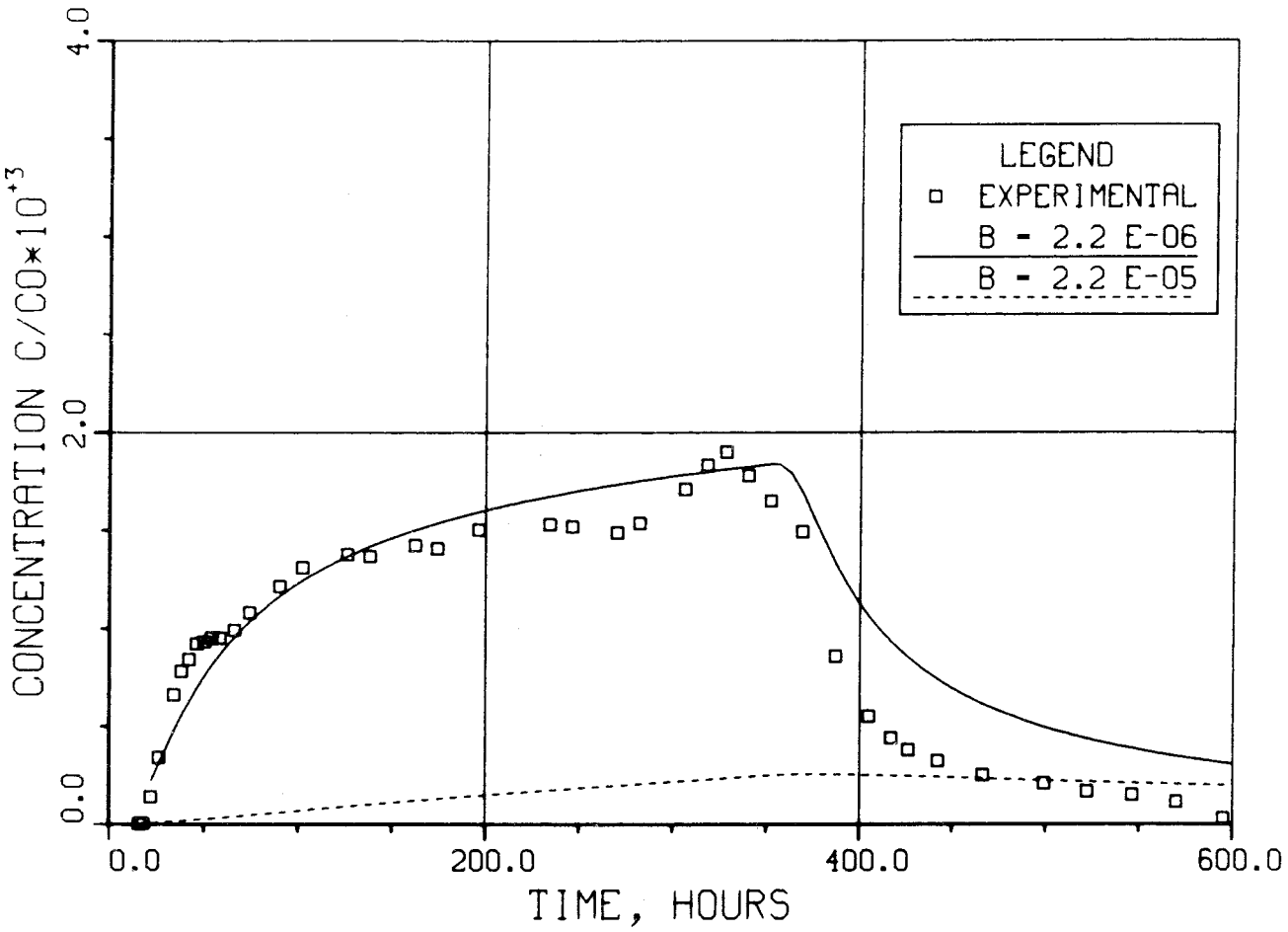

Figure 10.- Experimental data for strontium and curves calculated using the channeling dispersion-diffusion model, with the B-parameter determined by a fit (Table 6.8, column 2) and the B-parameter calculated from experimental measurements in the laboratory (Table 6.8, column 3).

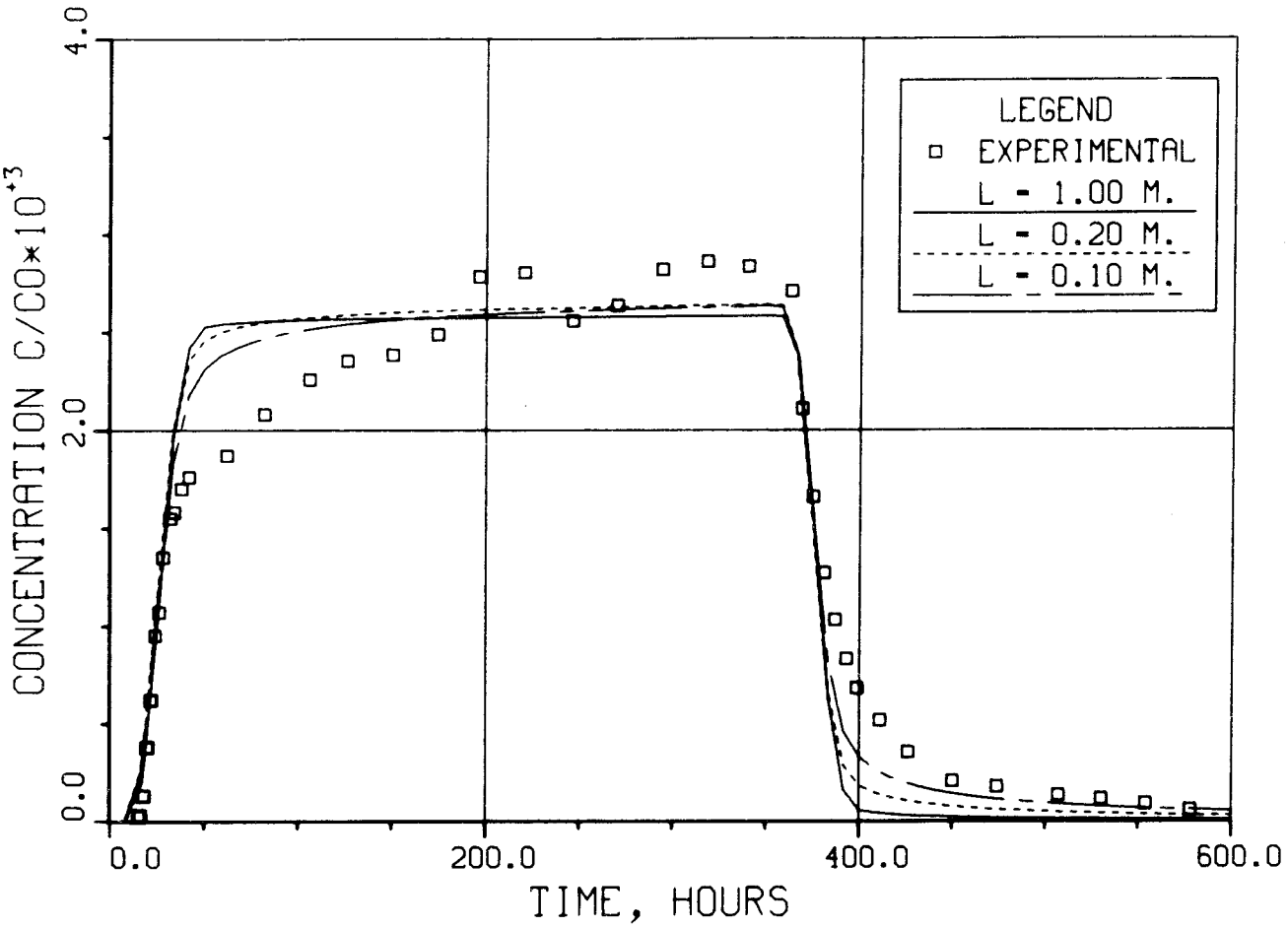

Figure 11.- Experimental data for iodide and calculated breakthrough curves using the hydrodynamic dispersion-diffusion and stagnant water model with different channels breadths for a Peclet number of 40 (Data from table 6.9).

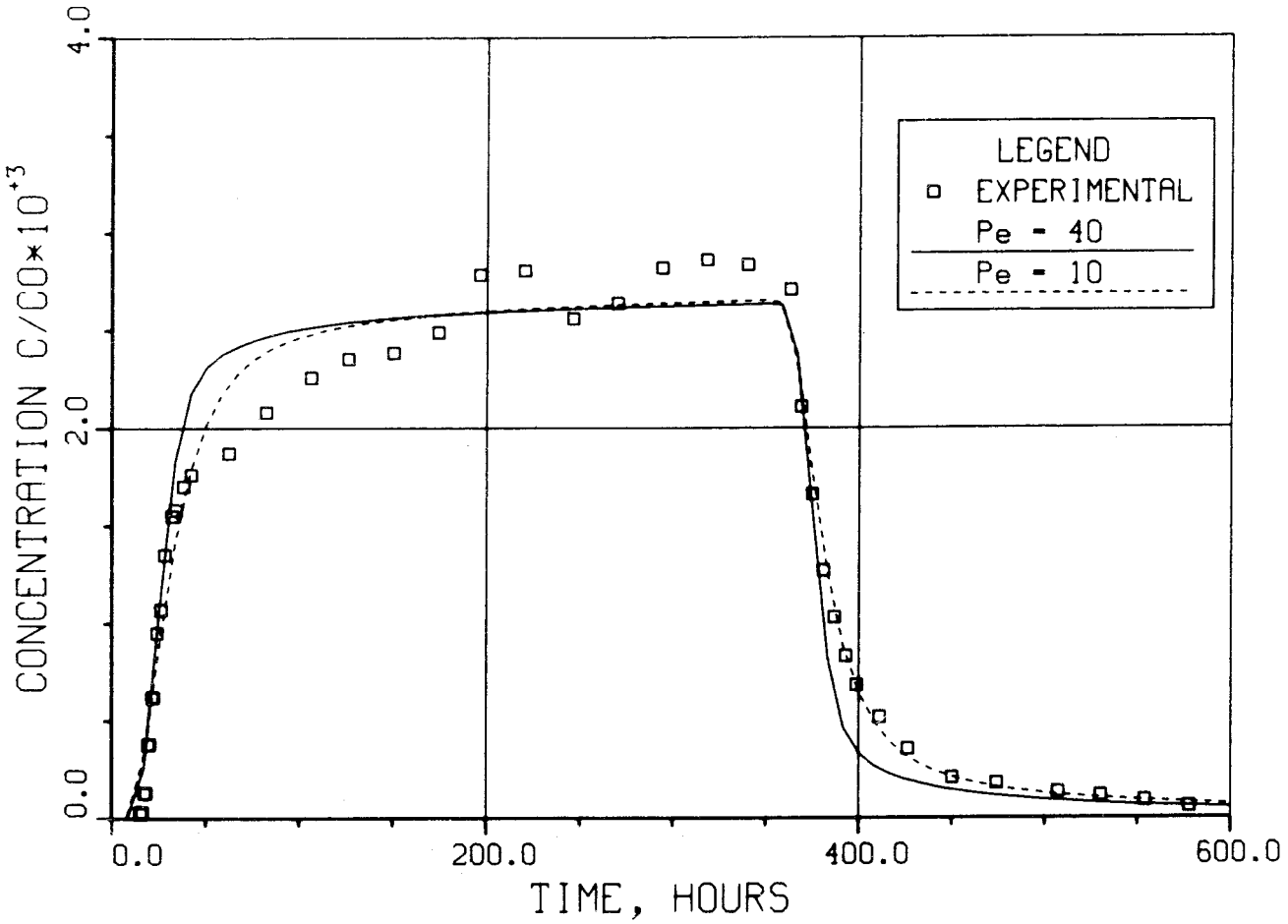

Figure 12.- Experimental data for iodide and calculated breakthrough curves using the hydrodynamic dispersion-diffusion and stagnant water model with different Peclet number for a channel breadth of 0.10 m (Data from table 6.9).

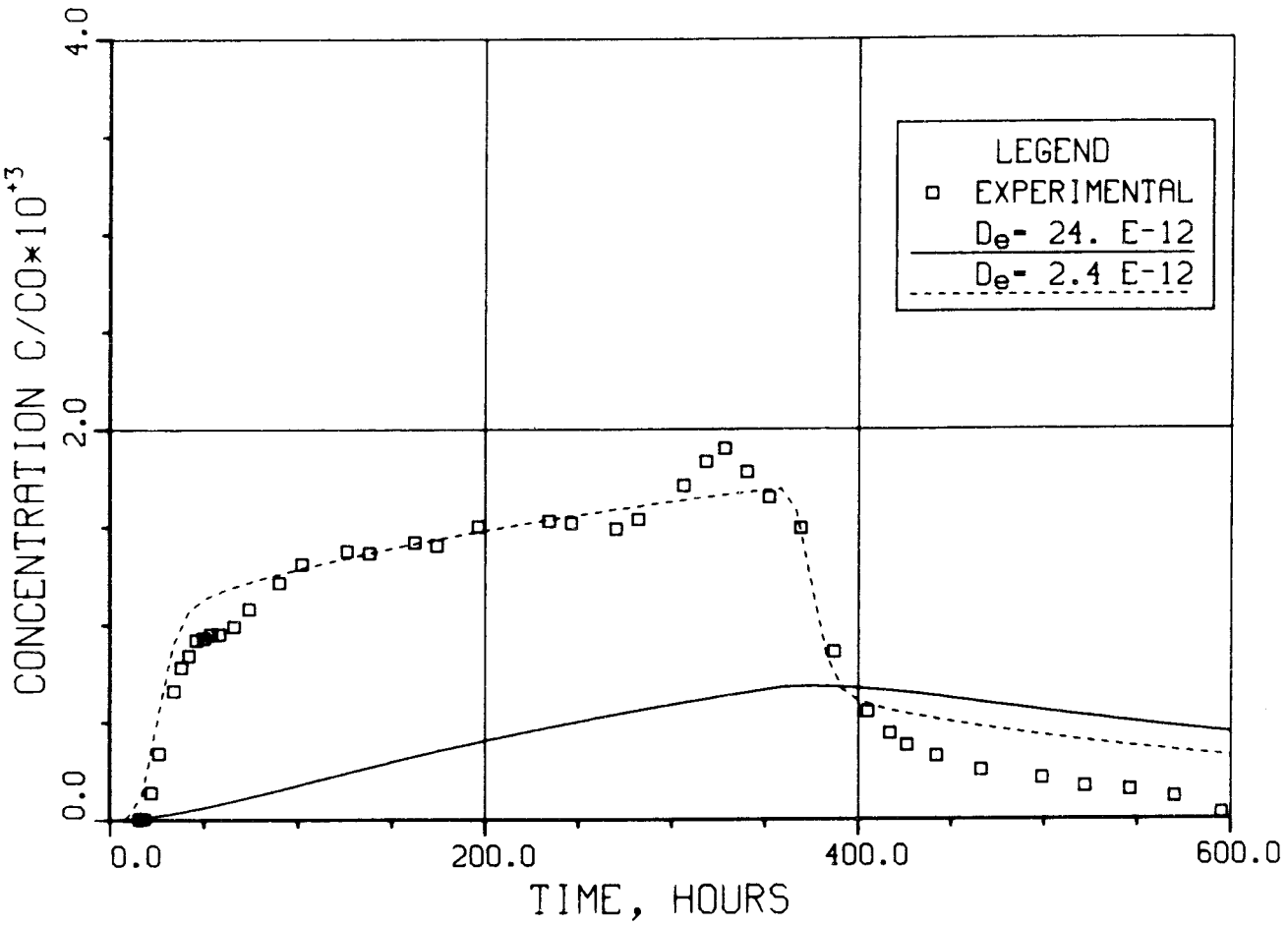

Figure 13.- Experimental data for strontium and calculated breakthrough curves using the hydrodynamic dispersion-diffusion and stagnant water model with different effective diffusivities.

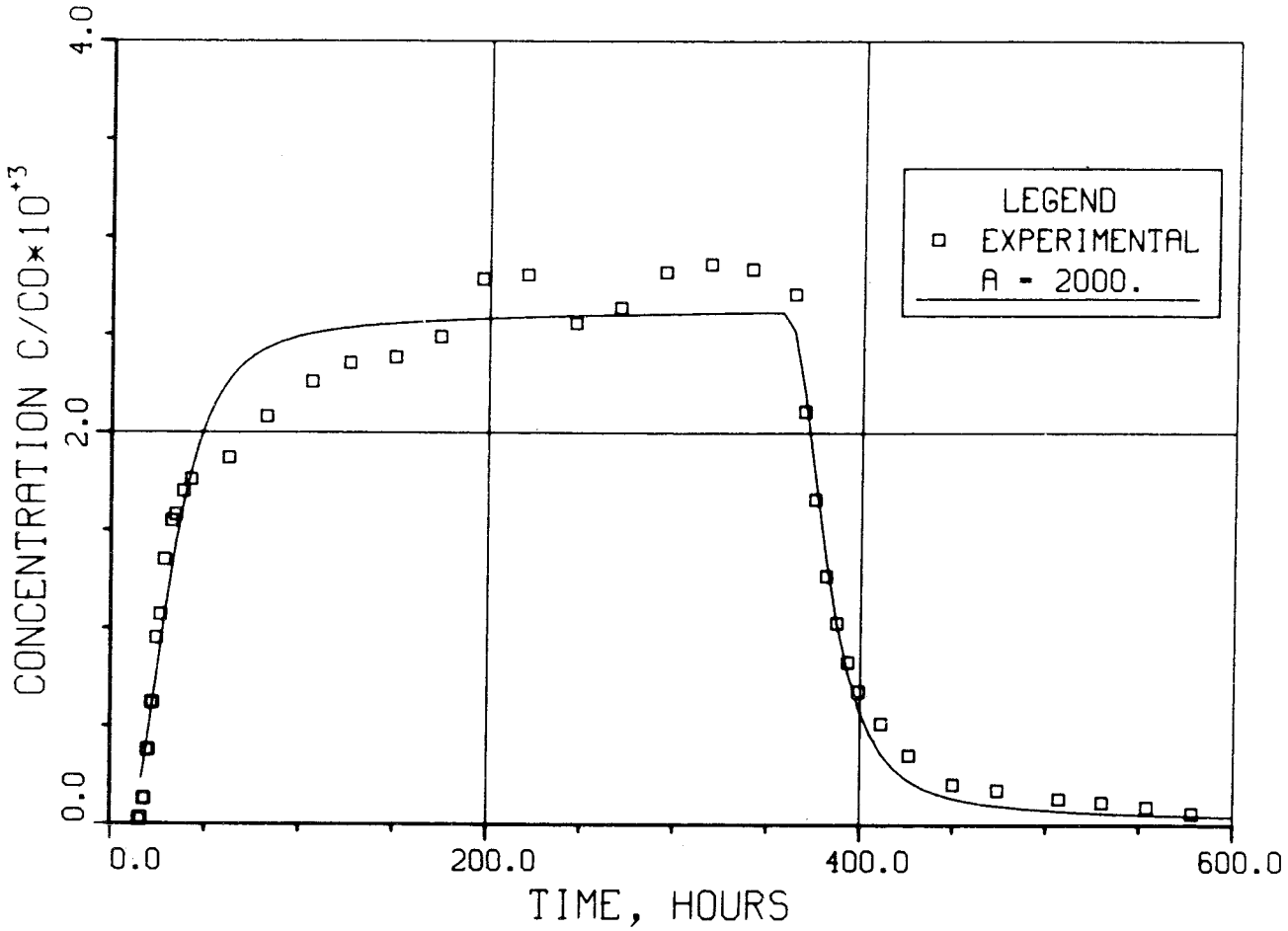

Figure 14.- Experimental data for iodide and fit using the hydrodynamic dispersion-diffusion model with the A-parameter determined from measurements in the laboratory in pieces of granite with coating material (Table 7.1, column 1).

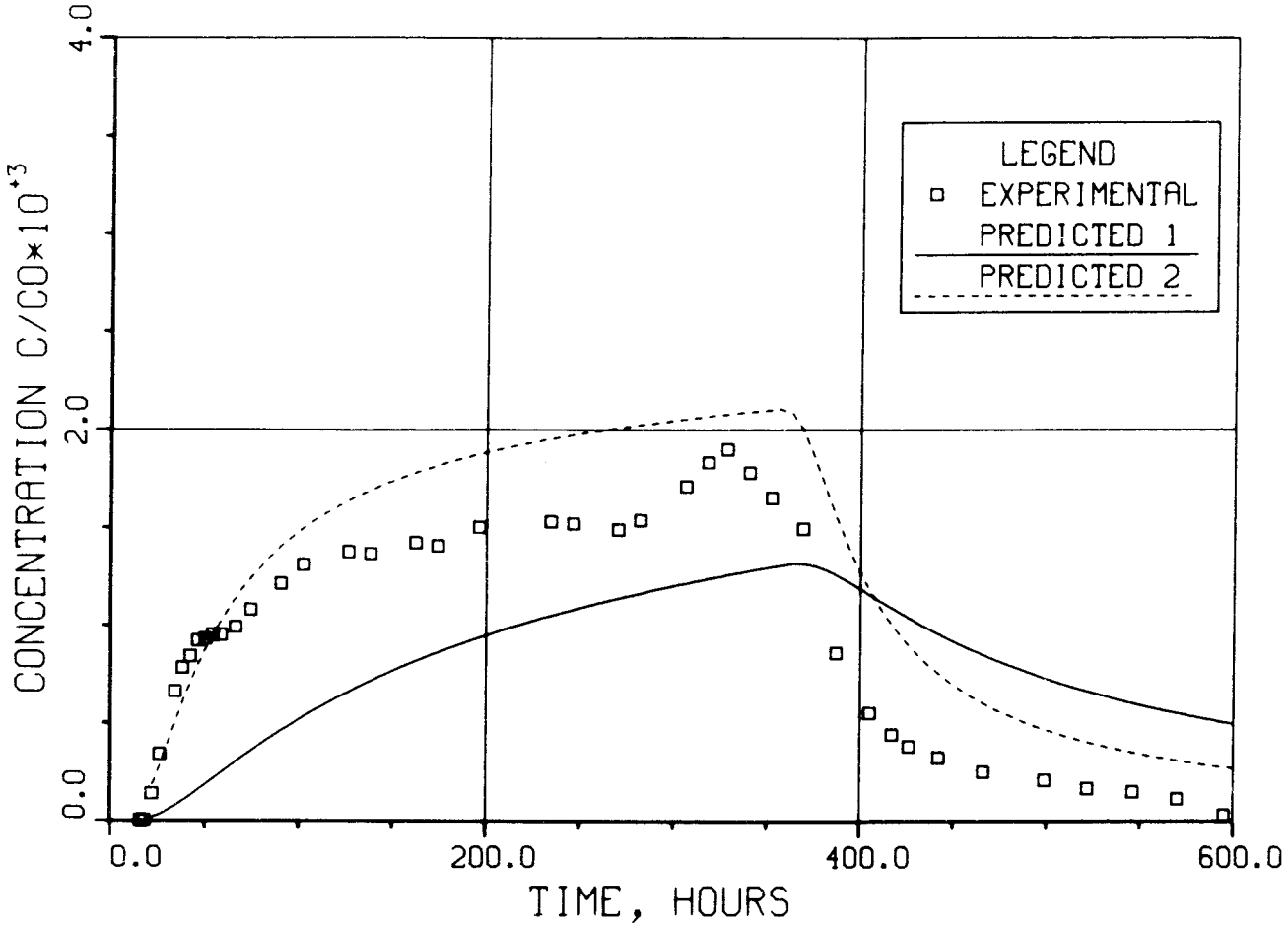

Figure 15.- Experimental data for strontium and predicted curves using the hydrodynamic dispersion-diffusion model. The curve 1 is calculated from values determined in sawed pieces of granite (Table 7.1, column 2).The curve 2 is determined considering the adsorption isotherm is nonlinear (Table 7.1, column 3) linearisation is used to get approximative solution.

LIST OF KBS's TECHNICAL REPORTS

1977-78

TR 121 KBS Technical Reports 1 - 120.
Summaries. Stockholm, May 1979.

1979

TR 79-28 The KBS Annual Report 1979.
KBS Technical Reports 79-01--79-27.
Summaries. Stockholm, March 1980.

1980

TR 80-26 The KBS Annual Report 1980.
KBS Technical Reports 80-01--80-25.
Summaries. Stockholm, March 1981.

1981

TR 81-17 The KBS Annual Report 1981.
KBS Technical Reports 81-01--81-16
Summaries. Stockholm, April 1982.

1983

TR 83-01 Radionuclide transport in a single fissure
A laboratory study
Trygve E Eriksen
Department of Nuclear Chemistry
The Royal Institute of Technology
Stockholm, Sweden 1983-01-19

TR 83-02 The possible effects of alfa and beta radiolysis
on the matrix dissolution of spent nuclear fuel
I Grenthe
I Puigdomènech
J Bruno
Department of Inorganic Chemistry
Royal Institute of Technology
Stockholm, Sweden January 1983

TR 83-03 Smectite alteration
Proceedings of a colloquium at State University of New York at Buffalo, May 26-27, 1982
Compiled by Duwayne M Anderson
State University of New York at Buffalo
February 15, 1983

TR 83-04 Stability of bentonite gels in crystalline rock - Physical aspects
Roland Pusch
Division Soil Mechanics, University of Luleå
Luleå, Sweden, 1983-02-20

TR 83-05 Studies in pitting corrosion on archeological bronzes - Copper
Åke Bresle
Jozef Saers
Birgit Arrhenius
Archaeological Research Laboratory
University of Stockholm
Stockholm, Sweden 1983-01-02

TR 83-06 Investigation of the stress corrosion cracking of pure copper
L A Benjamin
D Hardie
R N Parkins
University of Newcastle upon Tyne
Department of Metallurgy and Engineering Materials
Newcastle upon Tyne, Great Britain, April 1983

TR 83-07 Sorption of radionuclides on geologic media - A literature survey. I: Fission Products
K Andersson
B Allard
Department of Nuclear Chemistry
Chalmers University of Technology
Göteborg, Sweden 1983-01-31

TR 83-08 Formation and properties of actinide colloids
U Olofsson
B Allard
M Bengtsson
B Torstenfelt
K Andersson
Department of Nuclear Chemistry
Chalmers University of Technology
Göteborg, Sweden 1983-01-30

TR 83-09 Complexes of actinides with naturally occurring organic substances - Literature survey
U Olofsson
B Allard
Department of Nucluear Chemistry
Chalmers University of Technology
Göteborg, Sweden 1983-02-15

TR 83-10 Radiolysis in nature:
Evidence from the Oklo natural reactors
David B Curtis
Alexander J Gancarz
New Mexico, USA February 1983

TR 83-11 Description of recipient areas related to final storage of unreprocessed spent nuclear fuel
Björn Sundblad
Ulla Bergström
Studsvik Energiteknik AB
Nyköping, Sweden 1983-02-07

TR 83-12 Calculation of activity content and related properties in PWR and BWR fuel using ORIGEN 2
Ove Edlund
Studsvik Energiteknik AB
Nyköping, Sweden 1983-03-07

TR 83-13 Sorption and diffusion studies of Cs and I in concrete
K Andersson
B Torstenfelt
B Allard
Department of Nuclear Chemistry
Chalmers University of Technology
Göteborg, Sweden 1983-01-15

TR 83-14 The complexation of Eu(III) by fulvic acid
J A Marinsky
State University of New York at Buffalo, Buffalo,NY
1983-03-31

TR 83-15 Diffusion measurements in crystalline rocks
Kristina Skagius
Ivars Neretnieks
Royal Institute of Technology
Stockholm, Sweden 1983-03-11

TR 83-16 Stability of deep-sited smectite minerals in crystalline rock - chemical aspects
Roland Pusch
Division of Soil Mechanics, University of Luleå
1983-03-30

TR 83-17 Analysis of groundwater from deep boreholes in
Gideå Sif Laurent
Swedish Environmental Research Institute
Stockholm, Sweden 1983-03-09

TR 83-18 Migration experiments in Studsvik
O Landström
Studsvik Energiteknik AB
C-E Klockars
O Persson
E-L Tullborg
S Å Larson
Swedish Geological
K Andersson
B Allard
B Torstenfelt
Chalmers University of Technology
1983-01-31

TR 83-19 Analysis of groundwater from deep boreholes in Fjällveden
Sif Laurent
Swedish Environmental Research Institute
Stockholm, Sweden 1983-03-29

TR 83-20 Encapsulation and handling of spent nuclear fuel for final disposal
1 Welded copper canisters
2 Pressed copper canisters (HIPOW)
3 BWR Channels in Concrete
B Lönnerberg, ASEA-ATOM
H Larker, ASEA
L Ageskog, VBB
May 1983

TR 83-21 An analysis of the conditions of gas migration from a low-level radioactive waste repository
C Braester
Israel Institute of Technology, Haifa, Israel
R Thunvik
Royal Institute of Technology
November 1982

TR 83-22 Calculated temperature field in and around a repository for spent nuclear fuel
Taivo Tarandi
VBB
Stockholm, Sweden April 1983

TR 83-23

TR 83-24 Corrosion resistance of a copper canister for spent nuclear fuel
The Swedish Corrosion Research Institute and its reference group
Stockholm, Sweden April 1983

TR 83-25 Feasibility study of EB welding of spent nuclear fuel canisters
A Sanderson
T F Szluha
J Turner
Welding Institute
Cambridge, United Kingdom April 1983

TR 83-26 The KBS UO_2 leaching program
Summary Report 1983-02-01
Ronald Forsyth
Studsvik Energiteknik AB
Nyköping, Sweden February 1983

TR 83-27 Radiation effects on the chemical environment in a radioactive waste repository
Trygve Eriksen
Royal Institute of Technology
Stockholm, Sweden April 1983

TR 83-28 An analysis of selected parameters for the BIOPATH-program
U Bergström
A-B Wilkens
Studsvik Energiteknik AB
Nyköping, Sweden April 1983

TR 83-29 On the environmental impact of a repository for spent nuclear fuel
Otto Brotzen
Stockholm, Sweden April 1983

TR 83-30 Encapsulation of spent nuclear fuel - Safety Analysis
ES-konsult AB
Stockholm, Sweden April 1983

TR 83-31 Final disposal of spent nuclear fuel - Standard programme for site investigations
Compiled by
Ulf Thoregren
Swedish Geological
April 1983

TR 83-32 Feasibility study of detection of defects in thick welded copper
Tekniska Röntgencentralen AB
Stockholm, Sweden April 1983

TR 83-33 The interaction of bentonite and glass with aqueous media
M Mosslehi
A Lambrosa
J A Marinsky
State University of New York
Buffalo, NY, USA April 1983

TR 83-34 Radionuclide diffusion and mobilities in compacted bentonite
B Torstenfelt
B Allard
K Andersson
H Kipatsi
L Eliasson
U Olofsson
H Persson
Chalmers University of Technology
Göteborg, Sweden April 1983

TR 83-35 Actinide solution equilibria and solubilities in geologic systems
B Allard
Chalmers University of Technology
Göteborg, Sweden 1983-04-10

TR 83-36 Iron content and reducing capacity of granites and bentonite
B Torstenfelt
B Allard
W Johansson
T Ittner
Chalmers University of Technology
Göteborg, Sweden April 1983

TR 83-37 Surface migration in sorption processes
A Rasmuson
I Neretnieks
Royal Institute of Technology
Stockholm, Sweden March 1983

TR 83-38 Evaluation of some tracer tests in the granitic rock at Finnsjön
L Moreno
I Neretnieks
Royal Institute of Technology, Stockholm
C-E Klockars
Swedish Geological, Uppsala
April 1983

TR 83-39 Diffusion in the matrix of granitic rock
Field test in the Stripa mine. Part 2
L Birgersson
I Neretnieks
Royal Institute of Technology
Stockholm, Sweden March 1983

TR 83-40 Redox conditions in groundwaters from Svartboberget, Gideå, Fjällveden and Kamlunge
P Wikberg
I Grenthe
K Axelsen
Royal Institute of Technology
Stockholm, Sweden 1983-05-10

TR 83-41 Analysis of groundwater from deep boreholes in Svartboberget
Sif Laurent
Swedish Environmental Research Institute
Stockholm, Sweden April 1983

TR 83-42 Final disposal of high-level waste and spent nuclear fuel - foreign activities
R Gelin
Studsvik Energiteknik AB
Nyköping, Sweden May 1983

TR 83-43 Final disposal of spent nuclear fuel - geological, hydrological and geophysical methods for site characterization
K Ahlbom
L Carlsson
O Olsson
Swddish Geological
Sweden May 1983

TR 83-44 Final disposal of spent nuclear fuel - equipment for site characterization
K Almén, K Hansson, B-E Johansson, G Nilsson
Swedish Geological
O Andersson, IPA-Konsult
P Wikberg, Royal Institute of Technology
H Åhagen, SKBF/KBS
May 1983